Graduate School of Bioresources

Mie University

Ph.D. Thesis

Understanding the role of sea surface temperature variability in forcing regional precipitation variability in the rainy season in Mozambique

（モザンビーク各地における雨季降水量変動に対する海面水温強制の役割の理解）

Luis Adriano Chongue

September 2024

Contents

CHAPTER I 4

General Introduction 4

CHAPTER II 9

The influence of tropical and subtropical modes of climate variability on precipitation in Mozambique 9

1. Data 9

2. Results 10

3. Conclusions and Discussion 17

CHAPTER III 33

The Mozambique Channel trough variability and its influence on regional precipitation variability in Mozambique in austral summer 33

1. Data and Methodology 33

2. Results 34

3. Conclusion and Discussion 39

CHAPTER IV 48

General Conclusions 48

References 50

Abstract

This study examines the relationship between the interannual rainfall variability in the rainy season in Mozambique and global sea surface temperature (SST) fluctuations. Four geographical regions across Mozambique (southern, central, northeastern, and northwestern regions) are defined for the analysis. The relationship of December, January, and February (DJF) mean precipitation in those four regions with SSTs in the tropical and subtropical Atlantic, Pacific and Indian Oceans are investigated through lagged correlation and composite analysis.

The results suggest that interannual regional precipitation variability in Mozambique is modulated by several factors. The most important include the El Niño-Southern Oscillation (ENSO) in the tropical Pacific, the Benguela Nino in the Atlantic Ocean, the Indian Ocean Dipole (IOD) and the Subtropical Indian Ocean Dipole (SIOD) in the tropical and subtropical Indian Ocean. These modes of climate variability affect regional precipitation through modulating major regional weather systems. The Benguela Nino appears to modulate moisture flux from the Benguela coast into the Southern Indian Convergence Zone (SICZ) while ENSO modulates the strength of major regional systems such as Angolan law, Botswana High, Mascarene High and therefore, Inter Tropical Convergence Zone (ITCZ). On the other hand, although year to year variability of Mozambique Channel Trough (MCT) intensity is significantly correlated to ENSO, it does not accompany regional precipitation in Mozambique. However, its westward (eastward) shift, which is not significantly correlated to ENSO, accompanies enhanced (suppressed) precipitation in southern and central regions. This association is strengthened (weakened) when the westward (eastward) shift is accompanied by a positive (negative) phase of SIOD. We further found that Rossby wave propagation

reaching Southern Africa from the tropical Pacific is key to the relationship between precipitation in Mozambique and ENSO.

Benguela Niño was found to have a significant positive lead correlation by six months with precipitation in the southern, central, and northwestern regions. In contrast, the IOD led precipitation in the southern, central, and northeastern regions by three months. Overall, the modes of climate variability exerted stronger control over precipitation variability in southern and central Mozambique, and weaker control in northern Mozambique, particularly in the northwestern region.

CHAPTER I

General Introduction

Numerous studies have identified anomalies in sea surface temperatures (SSTs) in tropical and subtropical oceans that are responsible for interannual variability in precipitation in Southern Africa (Behera et al., 2018; Gaughan et al., 2016; Morioka et al. 2011; Mulenga et al. 2003; Pascale et al. 2019; Ratnam et al. 2014; Reason et al. 2006; Reason & Mulenga, 1999). These SST anomalies are associated with modes of climate variability, including El Niño Southern Oscillation (ENSO), Indian Ocean Dipole (IOD), Subtropical Indian Ocean Dipole (SIOD), and Benguela Niño (Jury & Huang, 2004; Nicholson, 2000).

Among all these modes of climate variability, ENSO is one of the most important determinants of year-to-year variability in precipitation over Southern Africa. La Niña events are generally linked to wetter conditions, whereas El Niño events are associated with drier conditions in Southern Africa during the rainy season (Camberlin et al., 2001; Kruger, 1999; McHugh, 2006; Meque & Abiodun, 2015, Reason & Jagadheesha, 2005; Ropelewski & Halpert, 1987). El Niño (La Niña) events can trigger Rossby wave propagation reaching to South Africa (Colberg et al. 2004), leading to weakening (deepening) of the Angolan Low over Southern Africa, and affecting precipitation variability there (Harp et al., 2021). However, the impact of ENSO on precipitation can differ from one location to another, even within South Africa (Rauniyar & Walsh, 2013). In addition, there is considerable diversity and nonlinearity in ENSO impacts on year-to-year precipitation variability over eastern Southern Africa (Blamey & Reason, 2023).

There are modes of climate variability other than ENSO that cause precipitation variability in Mozambique and other parts of Southern Africa. For example, there are two Indian Ocean Dipoles; IOD in the tropics and SIOD in the south (Behera & Yamagata, 2001; Saji et al., 1999). IOD is a major driver of climate, affecting precipitation during early austral summer (Moihamette, 2022). Although IOD can occur independently from ENSO, in years when they co-occur, ENSO variability has a significant impact on the IOD's periodicity, strength, and development processes (Behera et al., 2006). The positive phase of IOD is significantly associated with drier rainy seasons, whereas the negative phase is linked to wetter seasons in Southern Africa (Gaughan et al., 2016). However, the association between IOD and precipitation varies by region (Manatsa & Mukwada, 2012). The positive phase of SIOD is also generally linked to precipitation above normal levels in Southern Africa (Behera & Yamagata, 2001; Harp et al., 2021), however this relationship is susceptible to decadal variation (Behera et al., 2018).

Benguela Niño is a warm SST event that occurs in the eastern Atlantic Ocean near the frontal area between the southward-flowing Angola Current and the Benguela upwelling system off southwestern Africa (Florenchie et al., 2003; Imbol Koungue et al., 2017; 2019; Lübbecke et al., 2010; Shannon et al., 1986). This event generally leads to above-average precipitation in southwestern Africa, mainly over Angola and Namibia (Florenchie et al., 2003; Reason & Smart, 2015). Conversely, Benguela Niña, the cold phase, suppresses precipitation over there (Florenchie et al., 2003, Koseki & Koungue, 2020). However, the impacts of Benguela Niño and Benguela Niña on the precipitation can be modulated by ENSO and SIOD (e.g., Reason & Smart, 2015).

Mozambique is listed in the Global Climate Risk Index (GCRI) as one of the Southern African countries most vulnerable to interannual precipitation variability (Eckstein et al.,

2021). Severe events associated with precipitation variability, including droughts and floods, are recurrent in Mozambique, significantly affecting the country's economy, given its strong dependence on agriculture and natural resources. Additionally, similar to most African countries, Mozambique has a limited ability to adapt to climate change (Bozzola et al., 2018). Understanding precipitation variability in Mozambique is therefore crucial to ensure food security, prevent the outbreak of certain diseases, including cholera and malaria, and prevent natural disasters that result in loss of lives and property.

Despite its high vulnerability to weather-related loss events, few studies have examined inter-annual precipitation variability in Mozambique. Harp et al. (2021) studied the relationship between interannual variability of malaria outbreaks and climate in Mozambique and demonstrated that La Niña and positive SIOD lead to wetter conditions over southern Mozambique. Other studies have indicated that ENSO plays a crucial role in interannual precipitation variability in Mozambique, associating its warm phase (i.e., El Niño) with drier conditions and cold phases (i.e., La Niña) with wetter conditions (Machaieie et al., 2020; Manhique et. al., 2023, O'Brien & Vogel, 2003). However, the influence of modes of climate on interannual precipitation variability in Mozambique is not well understood.

The modes of climate variability modulate regional precipitation in Mozambique through modulation of Southern Africa regional weather systems such as the Angola Low (AL), Botswana High (BH), Mozambique Channel trough (MCT) (Driver and Reason 2017; Pascale et al. 2019; Barimalala et al. 2018, 2020), and Tropical Temperate Troughs (TTTs; Harrison, 1984; Washington and Todd, 1999; Manhique et al. 2011). While the influence of those regional systems on precipitation variability in Southern Africa has

been widely investigated, to our knowledge, few studies have focused on the MCT impact on the precipitation in Mozambique.

Figure 1a shows sea level pressure (SLP) and moisture flux averaged for December, January, and February (DJF) from 1981 to 2021 around the Mozambique Channel (MC). The MCT is a pronounced region of lower SLP associated with cyclonic circulation over the MC. Its formation is due to deflection of easterlies from the Indian Ocean by Madagascar's terrain (Barimalala et al. 2018). In addition to tropical cyclones (Mavume et al. 2009) and the intertropical convergence zone (ITCZ; Tyson and Preston-White 2000), the South Indian convergence zone (SICZ**;** Cook et al. 2000**)** plays a crucial role as the major precipitation driver in Southern Africa. The MCT influences precipitation variability in southern and central Mozambique by interacting with the SICZ and in northeastern Mozambique by influencing the Northeastern Indian Ocean monsoon (Barimalala et al. 2020).

The MCT exercises its influence mainly over the SICZ by modulating southwestward moisture flux from the Indian Ocean into the SICZ and therefore, increases precipitation over southern Africa, mainly in years with weak MCT (Barimalala et al. 2018). Furthermore, Pascale et al. (2019) pointed out the intensified moisture fluxes associated with the weakened MCT strengthened the Angola low and caused further increase in rainfall in the surrounding area.

While the rainy season in Mozambique is generally from October to March this study focused on precipitation averaged from December to February when mean precipitation is maximum and extreme precipitation events most often occur. The association of precipitation variability in each region of Mozambique with the modes of climate

variability of ENSO, IOD, SIOD, and Benguela Niño, were investigated in the first section, considering lagged effects and possible atmospheric teleconnections.

In the second section, this study focuses on the influence of year-to-year variability of the MCT on regional precipitation variability in Mozambique in austral summer. In addition to the variability in intensity, which has been already discussed in previous literature, that in zonal shift is also investigated. The findings of this study will be useful for improving seasonal predictions of regional precipitation in Mozambique.

CHAPTER II

The influence of tropical and subtropical modes of climate variability on precipitation in Mozambique

1. Data

We analysed monthly mean precipitation data for 1981−2021 from the Climate Hazards Research Group Infrared Precipitation with Stations (CHIRPS), which contains data spanning 50°S to 50°N (and all longitudes), with a horizontal resolution of approximately 5 km (Funk et al., 2015). This dataset results from the merging of ground station data with satellite estimations using observations of infrared cold cloud duration (Love et al., 2004) and provides a more complete and consistent time-series than meteorological station or satellite-based data alone. This is especially useful for Africa, where consistent ground station observations are lacking (Funk et al., 2015).

We used monthly SST, mean surface net long-wave radiation flux, 500-hPa geopotential height, 850-hPa specific humidity, 850- and 500-hPa meridional and zonal wind data from the ERA5 dataset, from the European Centre for Medium-Range Weather Forecast (ECMWF) with a spatial resolution of 0.25°× 0.25 ° (Hersbach et al., 2020).

The indices of modes of climate variability are defined as follows: ENSO was described using the Niño 3.4 index, which is based on area-averaged SST anomalies over 5°S–5°N and 170°W–120°W, and the Niño 1.2 index, calculated by averaging SSTs from 0°–10°S and 90°W –80°W. The Dipole Mode Index (DMI), an indicator of IOD, was calculated as the difference between area-averaged SSTs over the tropical western (10°S–0°, 50°E–70°E) and southeastern (10°S–0°, 90°E–110°E) Indian Ocean (Saji & Yamagata, 2003). The SIOD index was calculated as the area-averaged difference in SST between the

western (28°S –18°S, 55°E –65°E) and eastern (28°S –18°S, 90°E –100°E) subtropical Indian Ocean (Behera & Yamagata, 2001). The Benguela Niño index was determined as per Florenchie et al. (2003), who averaged SSTs from latitude 10°S –20°S and from longitude 8°E to the coast of southwest Africa. The ENSO phase of a particular season was based on the definition by the U.S. Climate Prediction Center (CPC), NCEP (https://origin.cpc.ncep.noaa.gov/products/analysis_monitoring/ensostuff/ONI_v5.phpht tps://origin.cpc.ncep.noaa.gov/products/analysis_monitoring/ensostuff/ONI_v5.php).

2. Results

We first examined 3-month mean precipitation during the rainy season in Mozambique from 1981 to 2021, to identify the peak of the climatological seasonal cycle of regional precipitation. The result suggests that December, January and February (DJF) mean is the season exhibiting highest precipitation mean values across Mozambique (Figure 1). The season was designated by the year in which the rainy season finished, e.g., season 1981 spans December 1980 to February 1981. Leading modes of year-to-year variability in DJF-mean precipitation across Mozambique (28°S–10°S, 30°E–42°E) was determined using the Empirical Orthogonal Function (EOF) analysis. DJF-mean precipitation was standardised by their standard deviations at every grid point prior to the EOF analysis. The first and second EOF modes had south-north dipole patterns, with the first and second explaining approximately 43% and 17% of the spatiotemporal variance, respectively (Figure 2). These results are consistent with Harp et al., (2021).

In Mozambique the weather forecast is provided according to the regional administrative divisions: southern, central, and northern regions. We used those divisions in conjunction with the EOF patterns to define four regions for area-averaged

precipitation: south (27°S–22°S, 31°E–36°E), central (21°S–16°S, 32°E–37°E), northwest (15°S–11.5°S, 34.5°E–37.5°E), and northeast (16°S–11°S, 38.5°E–41°E) (see red boxes in Figure 2a). Figure 3 shows the normalised time-series of DJF-mean precipitation averaged over each of the four regions. The normalized time series suggests that precipitation in the southern and central regions is significantly correlated. Although weaker, this is also valid for northeastern and northwestern regions. In fact, correlations of the former and latter are 0.68 ($p<0.001$) and 0.46 ($p<0.003$), respectively. In addition, precipitation in northern regions were negatively correlated with precipitation in the central and southern regions (not shown). These results are consistent with those of the EOF analysis (Figure 2). We mainly used precipitation in the southern region to represent southern and central regions while we used precipitation in the northeast to represent northeast and northwestern regions.

We first examined correlations between the southern, and northeastern time-series shown in Figure 3 with global SSTs during 1981−2021 (Figure 4). Consistently with Manhique et al., (2011), Gaughan et al., (2016), and Harp et al., (2021), precipitation in the southern region was positively correlated with SSTs in the equatorial western Pacific, and negatively correlated with SSTs over the central and eastern Pacific, indicating that precipitation in this region was negatively correlated with ENSO (Figure 4b). Negative correlation in the subtropical Southern Indian Ocean around 15°S and a positive correlation to the south around 30°S suggests that precipitation in the southern region of Mozambique is positively correlated with SIOD. Correlation of precipitation in the central region showed similar pattern (not shown). In contrast, precipitation in the northeastern region of Mozambique showed a positive but weaker correlation with ENSO and a negative correlation with SIOD (Figure 4a). However, that in the northwestern

region did not show significant correlation in most of oceans (not shown). Our results support ENSO as being the major climate mode associated with precipitation variability across all regions of Mozambique except for the northwest region.

To further investigate the association between ENSO and year-to-year variability in regional precipitation during the rainy season, we divided the rainy (DJF) seasons from 1981 to 2021 into three categories in each of the two regions: seasons with precipitation above-normal, seasons with normal precipitation, and seasons with below-normal precipitation. Precipitation above (below) normal was defined as being higher than 0.5 (lower than −0.5) standard deviation. In the southern region, the percentage of seasons with below-normal precipitation was 54% during El Niño, which was higher than that during La Niña or neutral ENSO, whereas seasons with above-normal precipitation were not observed during El Niño (Figure 5b). The categories with the highest percentage during La Niña and neutral ENSO were above normal and normal precipitation, respectively. These results are consistent with the negative correlation between ENSO and precipitation in the south. As for precipitation in the northeast, 46% of El Niño events were associated with above-normal precipitation, and 50% of La Niña events were associated with below-normal precipitation (Figure 5a), which is also consistent with weak negative correlation between ENSO and precipitation there.

Lead correlation coefficients of the indices of modes of climate variability with area-averaged DJF-mean regional precipitation are shown in Figure 6. The Niño 3.4 index, which represents ENSO, led to suppressed DJF-mean precipitation by three and six months (i.e., one and two seasons, respectively) in the southern (Figure 6a). IOD in leading SON was associated with more (less) precipitation in DJF in the northeastern region (southern region) (Figure 6b), consistently with Gaughan et al., (2016). Despite

showing significant simultaneous correlations with precipitation in the southern and northeastern regions, SIOD did not show significant correlation in leading seasons in any regions (Figure 6c). Benguela Niño led more (less) precipitation in the southern by two seasons (not shown). Although not shown with figures, lead correlations regarding precipitation in the central showed almost the same characteristic with that in the south. One exception is the Niño 1.2 index, which had negative lead correlation with precipitation in the central by one season but did not have correlation with precipitation in the south. In contrast, precipitation in the northwest did not show significant correlations with those climate modes except for Benguela Niña, which showed significant correlation in leading JJA.

We then investigated the association between large-scale atmospheric circulation anomalies and regional precipitation variability across Mozambique. Figures 7a and 7b show the composite differences of 500-hPa geopotential height between seasons with regional precipitation extremely above normal (an anomaly larger than 1 standard deviation) and those with precipitation extremely below normal (an anomaly less than –1 standard deviation), respectively. Used years are shown in Table 1. Precipitation in the south (shown with red boxes) was associated with a negative height (i.e., cyclonic) anomaly over South Africa and a positive height (i.e., anticyclonic) anomaly over the South Atlantic (Figure 7a). The cyclonic anomaly may be related to the weakening of the Botswana High (Driver & Reason, 2017). The wave-activity flux, as defined by Takaya & Nakamura (2001) and parallel to the group velocity of stationary Rossby waves, was northeastward between the cyclonic and anticyclonic anomalies, indicating that the Rossby wave train propagated from the South Atlantic to South Africa. This flux can be traced to the South Pacific in association with a chain of anticyclonic and cyclonic

anomalies over the South Atlantic, South America, and the South Pacific. A similar wave pattern was observed in the composite differences between La Niña and El Niño years (Figure 7c), suggesting that precipitation variability in southern Mozambique is linked to ENSO through this wave pattern. A similar wave pattern, but with much weaker amplitudes, was also associated with precipitation variability in the northeastern region (Figure 7b), consistent with the weak correlation with ENSO.

Although ENSO and regional precipitation variability in southern Mozambique were significantly correlated (Figure 6), there were some 'atypical' rainy seasons with normal precipitation even during El Niño or La Niña. To understand the difference between typical and atypical rainy seasons in south Mozambique, we created composite maps of circulation anomalies for El Niño seasons with extremely below-normal precipitation (i.e. typical El Niño seasons; Figure 8a), El Niño seasons with normal precipitation (atypical El Niño seasons; Figure 8b), La Niña seasons with extremely above-normal precipitation (typical La Niña seasons; Figure 8c), and La Niña seasons with normal precipitation (atypical La Niña seasons; Figure 8d). Composite maps were not created for El Niño seasons with above-normal precipitation or La Niña seasons with below-normal precipitation as there were a limited number of these events.

A Rossby wave train was observed from the South Pacific to an anticyclonic (cyclonic) anomaly over South Africa during typical El Niño (La Niña) seasons, with precipitation below (above) normal in association with the eastward wave-activity flux (Figure 8a, c). In atypical seasons, such an anticyclonic (cyclonic) anomaly over South Africa and cyclonic (anticyclonic) anomalies to the southwest were not observed even during El Niño (La Niña) seasons (Figure 8b, d), whereas circulation anomalies and associated wave-activity flux over the South Pacific during atypical seasons were similar to those

during typical seasons. This suggests that eastward propagation of a Rossby wave train over the South Pacific did not reach Southern Africa. The difference in the eastward propagation of the wave train should cause a difference in precipitation in the southern and central regions of Mozambique.

Composite maps were made as in Figure 8 but for OLR (Figure 9) and SST (Figure 10). During typical El Niño seasons, when precipitation is below normal, a negative OLR anomaly was over the central and eastern tropical Pacific, suggesting enhanced convective activity and upper-tropospheric anomalous divergence there, whereas a positive OLR anomaly was observed over the maritime continent (Figure 9a). These OLR anomalies were accompanied by cool SST anomalies over the central and eastern tropical Pacific and warm SST anomalies over the western tropical Pacific, which is typical during El Niño (Figure 10a). The OLR anomalies and associated upper-tropospheric divergence anomalies should be sources for the extratropical Rossby wave train that reaches South Africa (Figure 8a). In contrast, when precipitation is normal during atypical El Niño seasons, the OLR anomaly over the tropical Pacific is weaker than that during typical El Niño seasons (Figure 9b). The weaker OLR anomaly should also trigger a wave train, but its amplitude would be too weak to reach South Africa (Figure 8b), resulting in normal precipitation in southern Mozambique. The associated warm SST anomaly in the tropics in atypical El Niño seasons (Figure 10b) was slightly weaker than that in typical El Niño seasons, although the mean difference in the Niño 3.4 index between the two seasons is not statistically significant (Table 1). The OLR and SST anomalies in the tropics associated with La Niña can be observed in typical and atypical La Niña seasons (Figure 9c-d, 10c-d). These anomalies were weaker for atypical La Niña seasons, which may have resulted in the weaker wave train (Figure 8d). However, the mean difference in Niño 3.4

index between the two seasons was not statistically significant. The reason for the weaker Rossby wave propagation in atypical seasons should be future work.

For more detail discussion on the relationship of regional precipitation variability in Mozambique with major synoptic-scale weather systems affecting the seasonal cycle of precipitation in southern Africa such as the Inter Tropical Convergence Zone (ITCZ) (Tyson & Preston-White, 2000; Nicholson, 2018) and South Indian Convergence Zone (SICZ) (Cook, 2000; Ninomiya, 2008), composite maps for differences in moisture flux and OLR anomalies between seasons with regional precipitation extremely above normal and those with precipitation extremely below normal were made for each of two regions in Mozambique (Figure 11b,c). Increase of precipitation in the southern region accompanied enhanced moisture flux convergence and convective activity there associated with anomalies of the southwestward moisture flux from the Indian Ocean and the southeastward moisture flux from inland Africa (Figures 11b). In particular, the latter was originated over the southeastern Atlantic Ocean (not shown). This anomalous moisture flux convergence might activate tropical temperate troughs (TTTs) and SICZ, which are the main weather systems that bring precipitation variability in central and southern Mozambique (Manhique, et al., 2011). These anomalous moisture flux and convergence were clearer during typical La Nina seasons for the southern region (Figure 11a). In contrast, year-to-year precipitation variability in the northern regions is mainly due to the strength of the ITCZ, which is generally located over there during the summer season (Tyson & Preston-White, 2000). The enhanced precipitation in the northeastern regions was accompanied by the anomalous eastward moisture flux, which suggests weakening of westward moisture flux from the Indian Ocean in association with weakening of the Mascarene High (Figure 11c). In addition, the anomalous northward

moisture flux over the Mozambique Channel, which should accompany deepening of the Mozambique Channel trough (Barimanala *et al.,* 2020), caused enhanced moisture convergence to the north of 15ºS over northern Mozambique, along with enhanced eastward inland moisture flux from the Congo basin, flowing to northern Mozambique. These characteristics are consistent with the anomalous activity of the ITCZ over these regions.

3. Conclusions and Discussion

We defined four precipitation regions during the rainy season in Mozambique: southern, central, northwestern, and northeastern. Among these four regions, we mainly discussed precipitation in the southern and northeastern regions because that in the former (latter) correlates well with that in the central (northwestern) region. Focusing on the main rainy season (December, January and February), consistently with previous studies by Manhique et al., (2011), Gaughan et al., (2016) and Harp et al., (2021), we showed that precipitation above (below) normal in the central and southern regions tended to be associated with La Niña (El Niño) and the positive (negative) phase of SIOD, while associations between precipitation in the northwestern and northeastern regions and various modes of climate variability were relatively weak, particularly in the northwestern region. La Niña (El Niño), and negative (positive) phases of IOD tend to precede above- (below-) normal precipitation in central and southern regions of Mozambique by one season. The negative (positive) Niño 1.2 index tends to precede precipitation above (below) normal only in the central region by one season. With a lead time of two seasons, La Niña (El Niño) and positive (negative) phases of Benguela Niño exhibited robust associations with above- (below-) normal precipitation in southern and central regions.

The correlation with IOD was maximum in leading SON but it was not significant in DJF (Figure 6b). This might be because the IOD-related SST anomalies in the tropical Indian Ocean are the maximum around September and October and decline rapidly subsequently (Saji et al. 1999).

The northwestern and northeastern regions were less affected by modes of climate variability. Positive (negative) IOD in preceding SON season was significantly associated with precipitation above (below) normal in the northeastern region. Our results are consistent with that of Gaughan et al., (2016), who examined precipitation variability for October to April from 1921 to 2014 and found a correlation between IOD and precipitation in northern Mozambique. In the northwestern region, only the negative (positive) phase of Benguela Niño was significantly associated with precipitation above (below) normal with a lead time of two seasons.

Our results also correspond well with those of Driver & Reason (2017), who found that excessive precipitation in southern and central Mozambique is generally linked to a cyclonic anomaly of geopotential height in the middle troposphere over South Africa (i.e., weakening of the Botswana High). This cyclonic anomaly was accompanied by an anticyclonic anomaly to the southwest over the South Atlantic Ocean indicating that these circulation anomalies develop with incoming Rossby wave propagation from the tropical Pacific through the South Pacific and South Atlantic. La Niña events tend to accompany such wave propagation, consistent with the tendency of excessive precipitation in southern and central Mozambique during La Niña. In contrast, below-normal precipitation in the southern and central regions tends to accompany El Niño through Rossby wave propagation similar to that of La Niña, but with opposite phase. Our results are also consistent with those of previous studies by Gaughan et al., (2016), Harp et al.,

(2021), and Machaieie et al., (2020). Our novel finding is that even in atypical La Niña and El Niño events, which did not accompany precipitation anomalies in southern and central Mozambique, there was also Rossby wave propagation over the South Pacific as in typical ENSO events, but it did not reach the South Atlantic and South Africa.

Although the precipitation in the central region had high correlation with that in the southern region, a composite map of 500-hPa height anomalies for La Niña seasons with extremely above-normal precipitation (i.e., typical La Niña seasons) in the central region shows that an anticyclonic anomaly over the South Atlantic, which was observed in typical La Niña seasons for southern region (Figure 9c), was weaker (not shown). This is also true for atypical La Niña seasons. This result suggests that precipitation in the central region during La Niña is not necessarily regulated by the strength of the Rossby wave train, but rather by other factors like tropical cyclones (Mavume et al., 2009). In fact, tropical cyclones such as Berola in January 1996, Lisette in February 1997, Beltane in February 1998, Eline in February 2000, Cyprien in December 2001 and Chalane in December 2020 reached the central region of Mozambique during La Niña seasons with precipitation above normal there. (https://meteofrance.re/fr/cyclone).

Composited anomalies of moisture flux and OLR suggested that excessive precipitation in the southern and central regions might be contributed to by the variability of TTTs and SICZ through anomalous moisture transport from the Indian Ocean and inlaid Africa with origin in the southeast Atlantic Ocean mainly during La Niña seasons. Our results are consistent with those of Manhique et. al., (2015) who studied extreme precipitation event of 2013, under Benguela Niño, in Southern Africa and found their association with TTTs and SICZ systems. In the northern regions, the precipitation might be intensified by the enhanced ITCZ over there, particularly during El Niño seasons

accompanied by negative SIOD. This enhancement should be associated with that of the Mascarene High and the Mozambique Channel trough (Barimalala et al., 2022; Reason & Mulenga, 1999).

Although we demonstrated that seasons with above-normal precipitation in the northern regions tended to be associated with Rossby wave propagation, particularly in the northeastern region, but with much weaker amplitudes compared to those accompanied by precipitation anomalies in southern and central regions. We need more study to find factors that cause year-to-year precipitation variabilty there for better skill of the seasonal forecast. Furthermore, the 40 years of precipitation data used in this study may not be sufficient to draw clear conclusions. Examination of additional factors that may affect precipitation variability in Mozambique using longer-term observational datasets or the output of climate model experiments, is required to confirm the relationships observed in our study.

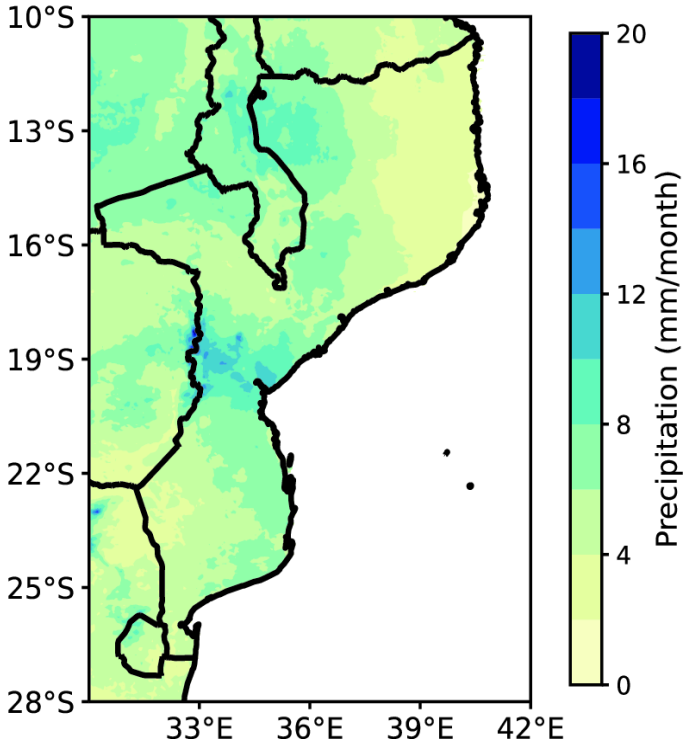

FIGURE 1 Mean precipitation (1981-2021; mm per month) in Mozambique for DJF.

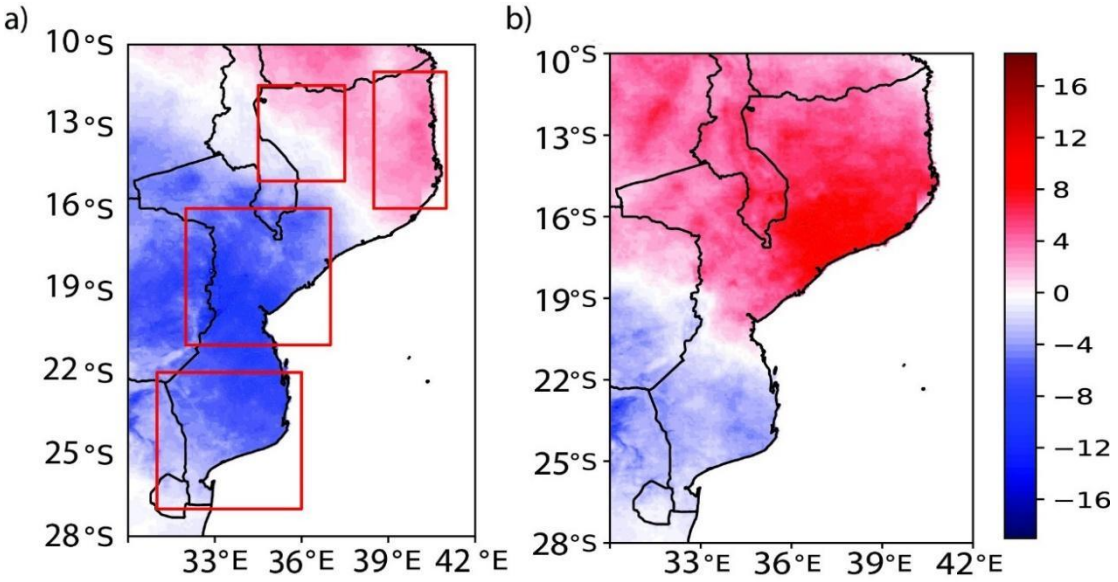

FIGURE 2 Spatiotemporal variability in summer in Mozambique, 1981−2021: (a) First mode (EOF1) for DJF, (b) Second mode (EOF2) for DJF. (Arbitrary units)

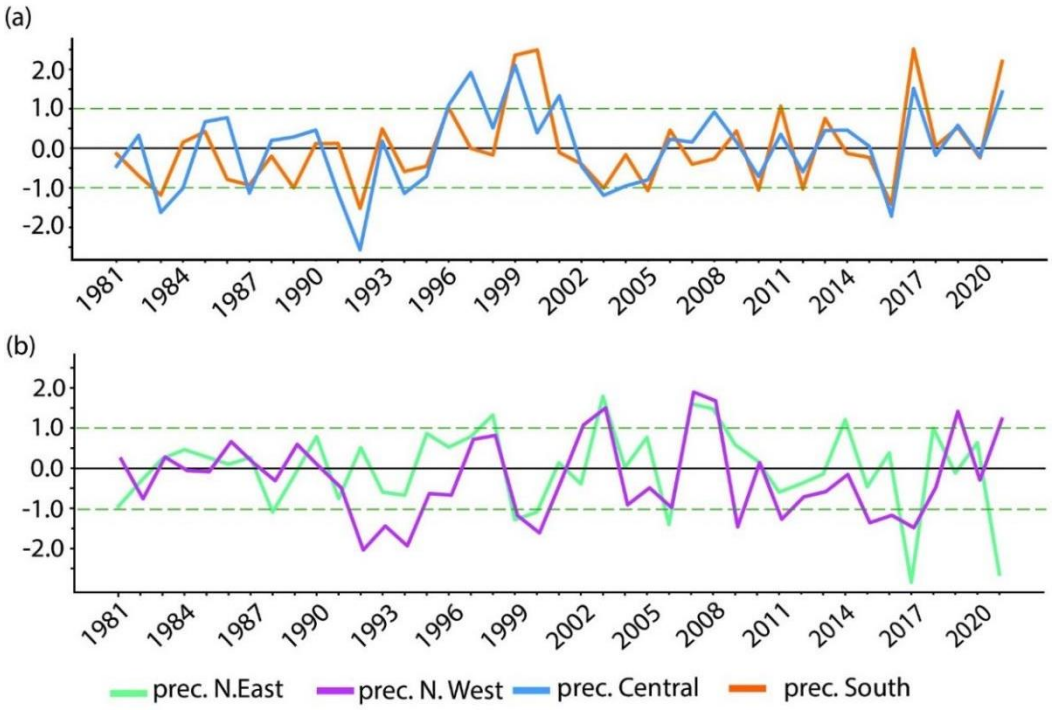

FIGURE 3 Regional time-series of normalised precipitation from 1981 to 2021 for DJF mean. (a) southern (orange line) and central (blue) regions, and (b) northwestern (green) and northeastern (pink) regions. Horizontal dashed lines correspond to –1 and +1 standard deviations.

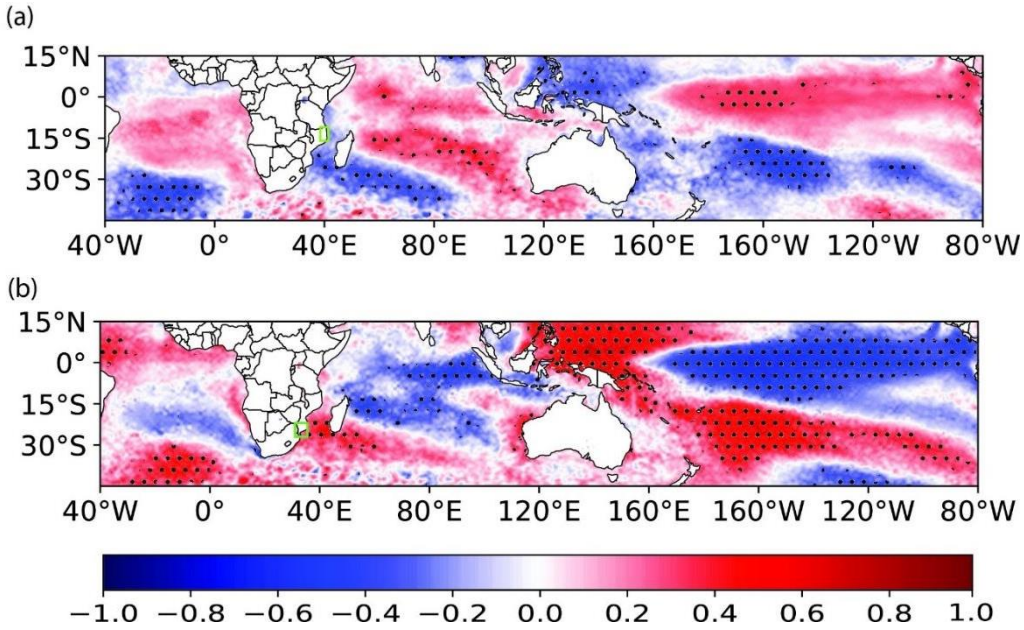

FIGURE 4 Maps of correlation coefficients between area-averaged precipitation in the two areas of Mozambique (green box) and global SSTs for DJF, 1981−2023: (a) northeastern region, (b) southern region. Black dots indicate statistically significant correlation at the 5% level.

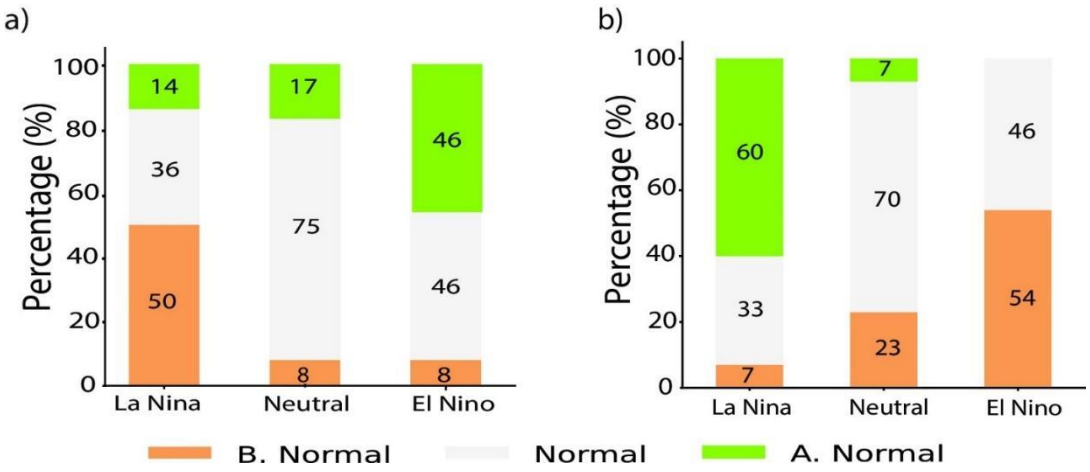

FIGURE 5 Percentages of seasons with precipitation below normal (orange), normal (white), and above normal (green), during each of three ENSO phases in summer (DJF), 1981-2023) in (a) northeastern and (b) southern regions of Mozambique.

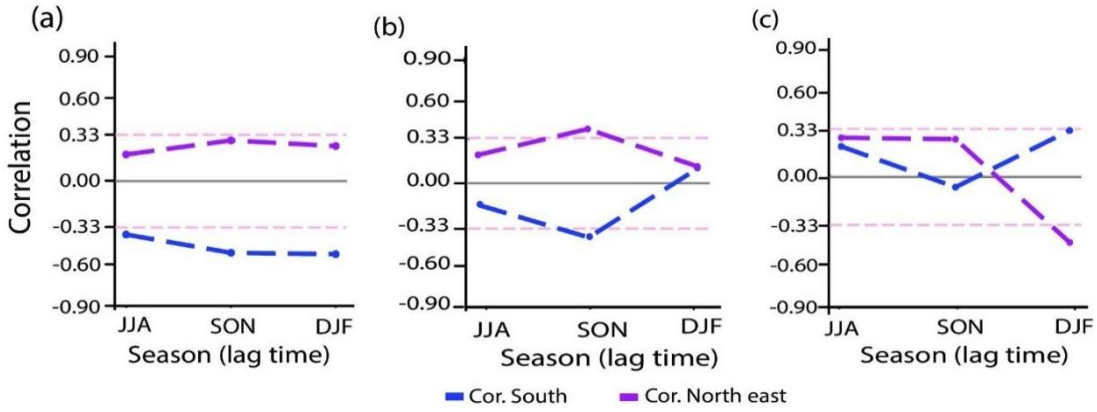

FIGURE 6 Time-lag correlation coefficients between regional precipitation and modes of climate variability of (a) Niño 3.4, (b) IOD, and (c) SIOD. DJF is the pivot season. JJA and SON represent one and two leading seasons relative to DJF. Upper and lower horizontal brown dashed lines represent the correlation being significant at the 5% level.

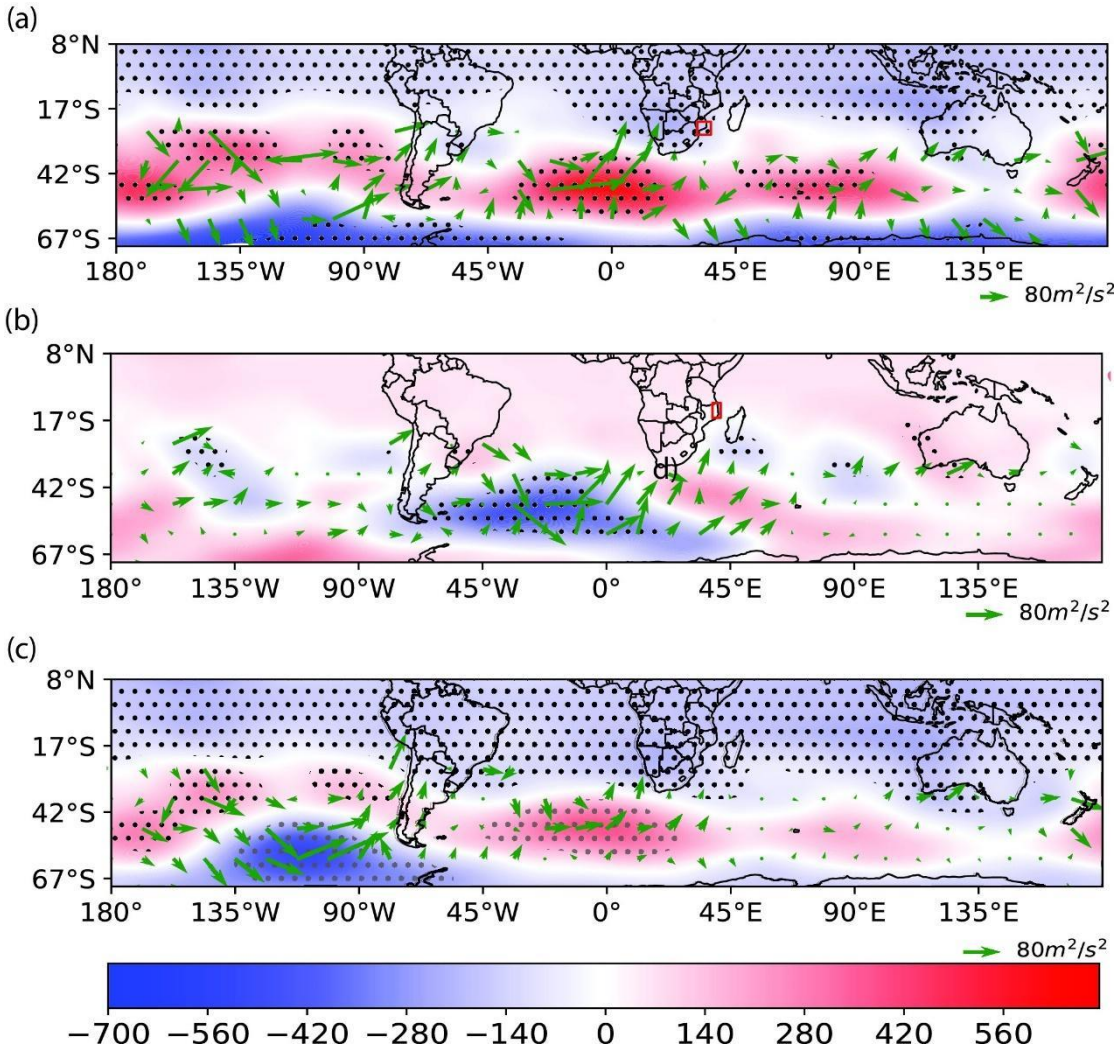

FIGURE 7 DJF composited difference of 500-hPa geopotential (in metres, shading) between years with precipitation extremely above normal and those with precipitation extremely below normal in the two regions of Mozambique: (a) southern region and (b) northeastern region. (c) Same as in (a) but for difference between La Niña and El Niño years. Black dots indicate a statistically significant difference at the 10% level. Arrows indicate the wave-activity flux ($m^2\ s^{-2}$).

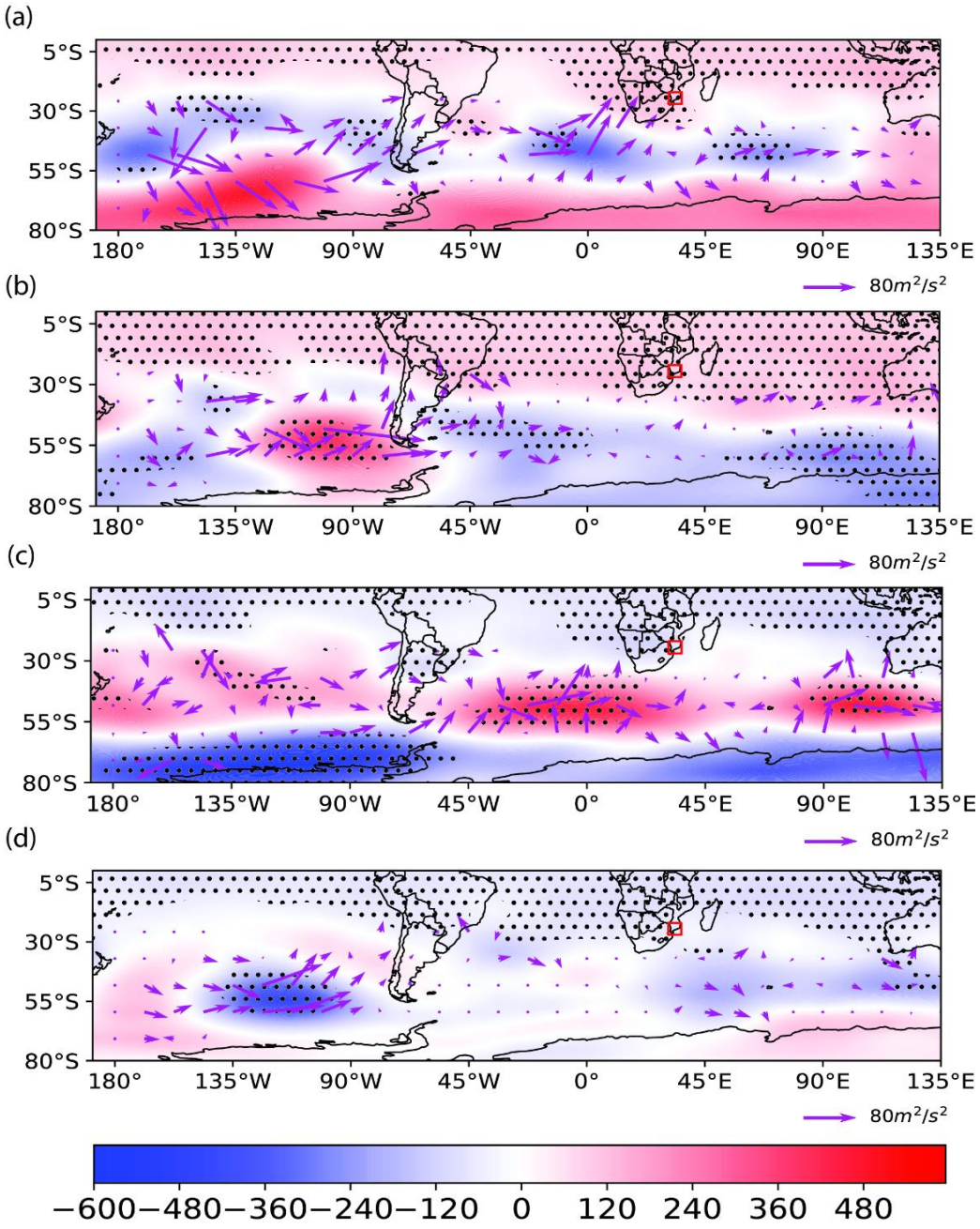

FIGURE 8 (a) Composited anomalies of 500-hPa geopotential (m^2 s^{-2}, shading) for El Niño years with precipitation below normal in southern Mozambique in DJF. The unit is m. Black dots show a statistically significant difference at the 10% level. Arrows indicate the wave-activity flux (m^2 s^{-2}). (b) As in (a) but for El Niño years with normal precipitation. (c) As in (a) but for La Niña years with precipitation above normal. (d) As

in (a) but for La Niña years with normal precipitation.

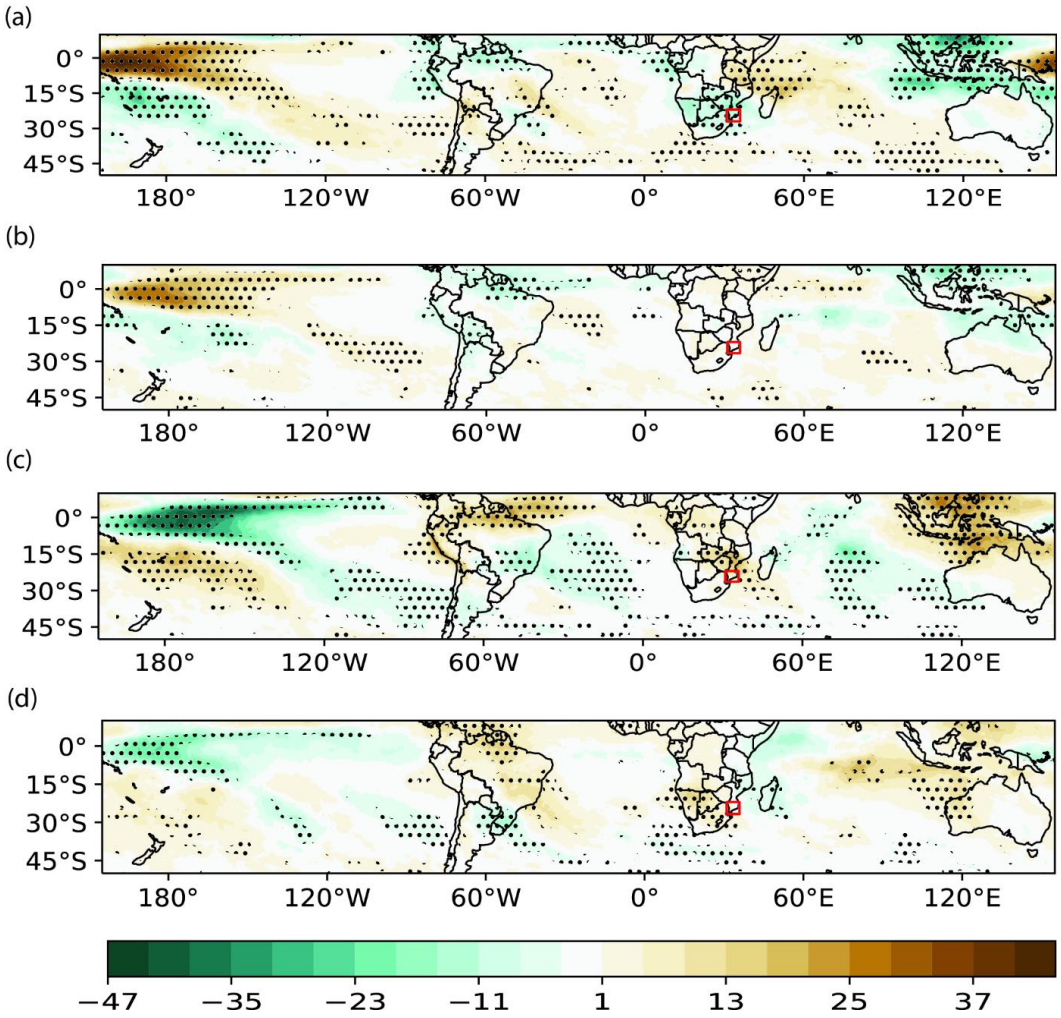

FIGURE 9 Same as Figure 8, but for Outgoing Long Wave Radiation (OLR; Wm^{-2}).

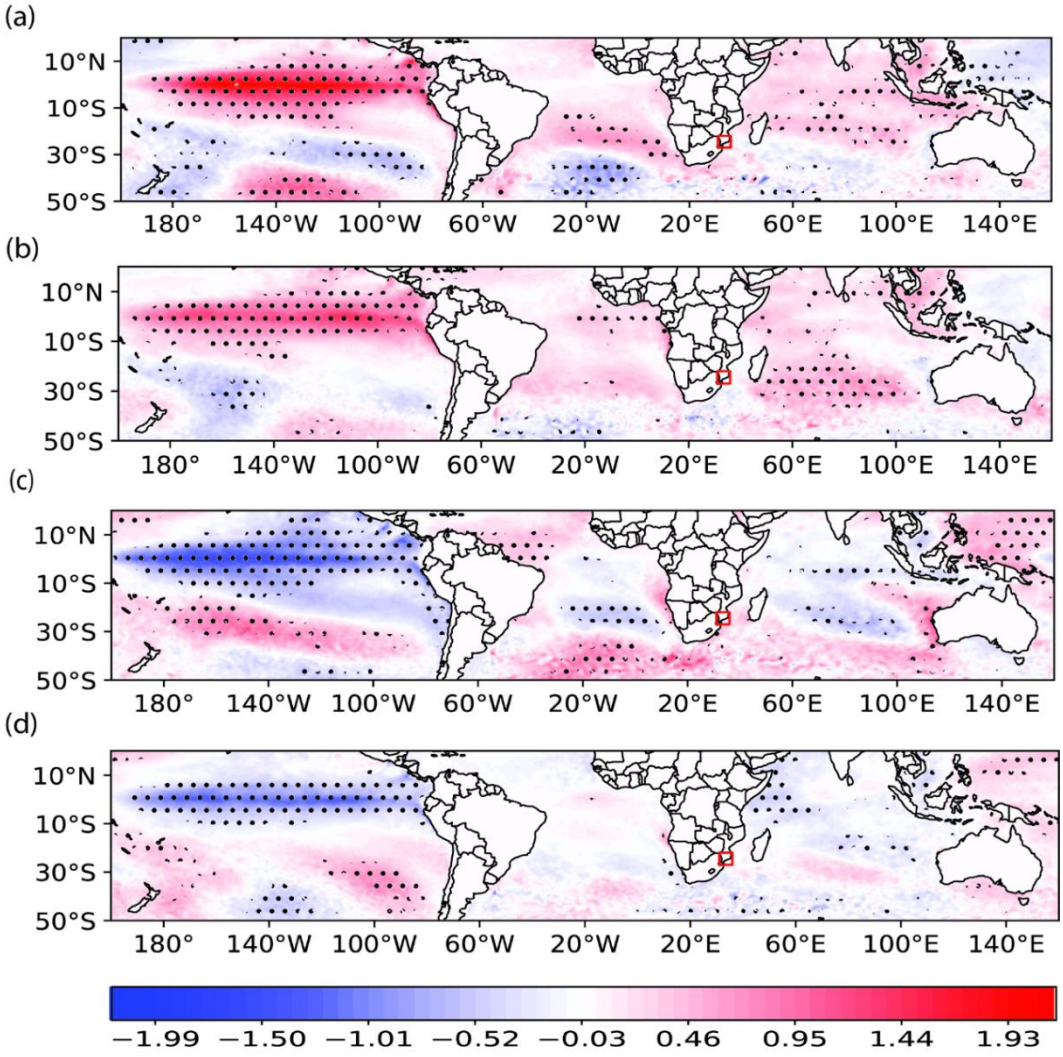

FIGURE 10 Same as in Figure 8, but for SST. The unit is K.

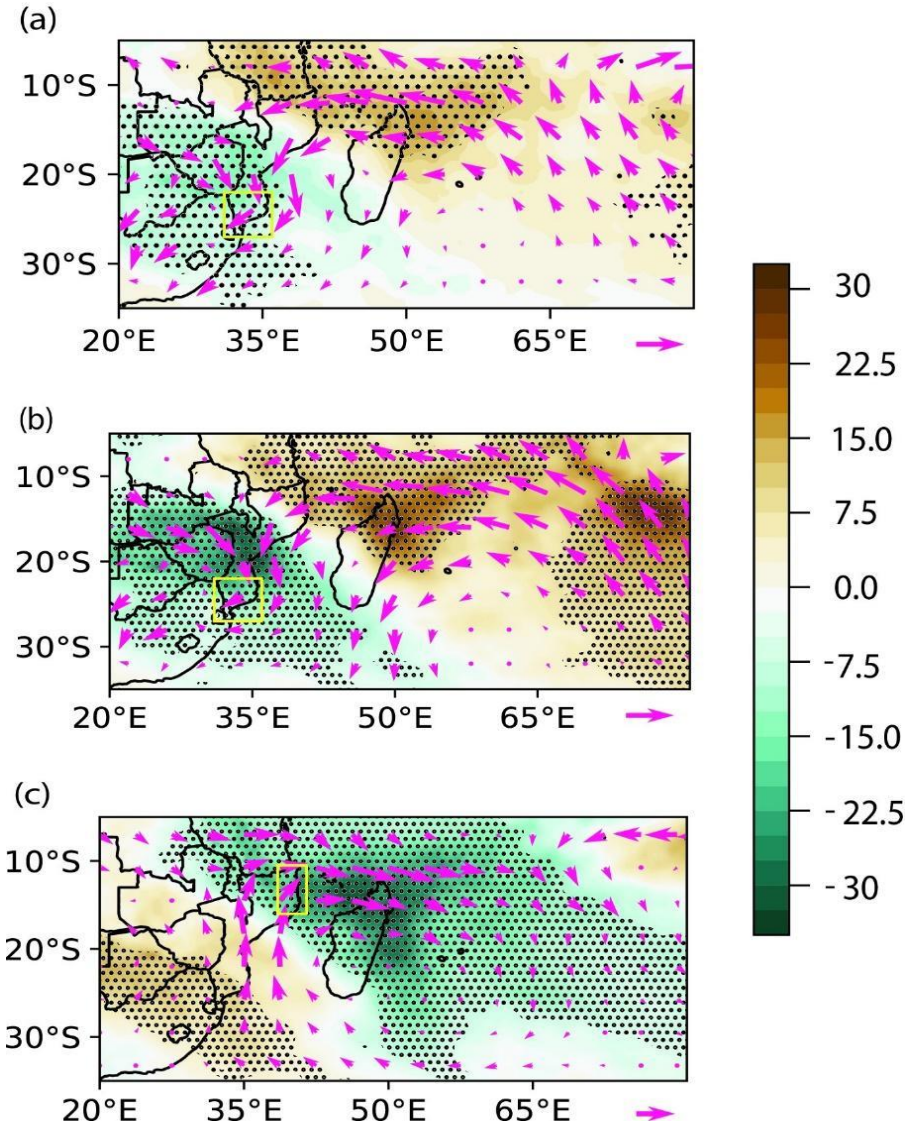

FIGURE 11 Composited anomalies of 850-hPa moisture flux (10^{-5} Kg m^{-2} s^{-1}, pink arrows) and outgoing long wave radiation (W m^{-2}, shading) for La Niña seasons with precipitation above normal in south (a), and the composited difference between years with precipitation above normal and those with precipitation below normal in the two regions of Mozambique: (b) southern region, and (c) northeastern region. Black dots show a statistically significant difference at the 10% level.

	Years
Rainfall extremely above normal in the south	1996, 1999, 2000, 2011, 2017, 2021
Rainfall extremely below normal in the south	1983, 1992, 2003, 2005, 2010, 2016
Rainfall extremely above normal in the central	1996, 1999, 2001, 2008, 2017, 2021
Rainfall extremely below normal in the central	1983,1987, 1992, 1994, 2003, 2016
Rainfall extremely above normal in the northwest	1989, 1991, 1999, 2002, 2003, 2019, 2021
Rainfall extremely below normal in the northwest	1990, 1992, 1998, 2005, 2015, 2017, 2020
Rainfall extremely above normal in the northeast	1991, 1993, 1995, 2003, 2007, 2008, 2014
Rainfall extremely below normal in the northeast	1983, 1988, 1998, 2000, 2009, 2013, 2021
La Niña years	1984, 1985, 1989, 1996, 1999, 2000, 2001, 2006, 2008, 2009, 2011, 2012, 2018, 2021
El Niño years	1983, 1987, 1988, 1992, 1995, 1998, 2003, 2005, 2007, 2010, 2015, 2016, 2019
La Niña years with precipitation above normal	1996(-0.9), 1999(-0.9), 2000(-1.7), 2009(-0.8), 2011(-1.4), 2021(-1)
La Niña years with normal precipitation	1984(-0.6), 1985(-1), 2001(-0.7), 2008(-1.6), 2009(-0.8), 2018(-0.9)
El Niño yeas with precipitation below normal	1983(2.2), 1987(1.2), 1992(1.7), 1995(1.0), 2003(0.9), 2005(0.6), 2010(1.5), 2016(2.5)
El Niño years with normal precipitation	1988(0.8), 1995(1), 1998(2.2), 2007(0.7), 2015(0.5), 2019 (0.7)

TABLE 1 Years used for the composite analysis. Values in brackets indicate the Niño 3.4 index.

CHAPTER III

The Mozambique Channel trough variability and its influence on regional precipitation variability in Mozambique in austral summer

1. Data and methodology

1.1 Data

We used monthly data of sea surface temperature (SST), 500-hPa geopotential, 850-hPa specific humidity, 850-hPa meridional and zonal wind, and SLP from the ERA5 reanalysis provided by European Centre for Medium-Range Weather Forecast (ECMWF) (Hersbach et al. 2020). The period is from 1981 to 2021 and the horizontal resolution is 0.25°× 0.25°. We also analyzed monthly mean precipitation data for the same period, from the Climate Hazards Research Group Infrared Precipitation with Stations (CHIRPS), which contains data spanning 50°S to 50°N (and all longitudes), with a horizontal resolution of approximately 5 km (Funk et al. 2015). El Niño Southern Oscillation (ENSO) was described using the Niño 3.4 index taken from U.S. Climate Prediction Center (CPC), NCEP (https://origin.cpc.ncep.noaa.gov/products/analysis_monitoring/ensostuff/ONI_v5.php), while the SIOD index was calculated as the area-averaged difference in SSTs between the western (28°S –18°S, 55°E –65°E) and eastern (28°S –18°S, 90°E –100°E) subtropical Indian Ocean (Behera and Yamagata 2001).

We defined four regions for area-averaged precipitation in Mozambique to evaluate regional precipitation variability. These are south (27°S–22°S, 31°E–36°E), central (21°S–16°S, 32°E–37°E), northwest (15°S–11.5°S, 34.5°E–37.5°E), and northeast (16°S–11°S, 38.5°E–41°E) regions in Mozambique. This is because the weather forecast

is provided according to these regional administrative divisions (e.g., Chongue and Nishii, 2024).

1.2 Methodology

Considering that DJF-mean precipitation in Mozambique, particularly in its central and southern regions, is the largest (Chongue and Nishii, 2024), we applied the empirical orthogonal function (EOF) analysis for year-to-year variability of DJF-mean SLP around the center of the MCT (16–26°S, 35–44°E) to evaluate the MCT variability. Before the analysis, we standardized SLP by their standard deviations at every grid point. The first EOF mode explains approximately 88% of the spatiotemporal variance and has a monopole pattern (Fig. 1b), suggesting year-to-year variability of the MCT intensity. The second mode explains 9% and has an east-west dipole pattern (Fig. 1c), suggesting zonal shift of the MCT relative to its climatological position. We hereafter refer to the principal component of the first (second) EOF mode as PC1_SLP (PC2_SLP).

It should be noted that Barimalala et al. (2020) focused on the MCT intensity during January, February and Mach (JFM) when is the seasonal peak of its intensity and tested several definitions for the MCT intensity. We will discuss the differences of our definition from them in the discussion.

2. Results

Table 1 shows correlation of PC1_SLP and PC2_SLP with regional precipitation in Mozambique. It is noteworthy that PC1_SLP is not correlated to the precipitation in all four regions in Mozambique whereas PC2_SLP is significantly correlated to those except

for the northwestern region. ENSO and SIOD significantly modulate precipitation in Mozambique (e.g., Chongue and Nishii, 2024), thus we also computed correlations of MCT variability with modes of climate variability. PC1_SLP is negatively and significantly correlated with the Niño 3.4 index but does not have a significant correlation with the SIOD index. In contrast, PC2_SLP is not significantly correlated with the Niño 3.4 index but has significant correlation with the SIOD index.

It's worth noting that the significant correlation between the MCT intensity and ENSO is mainly due to a strong association of El Niño years with weakened MCT (Fig. 1e). La Niña does not control the MCT intensity. Likewise, significant correlation between the precipitation in the south and ENSO is mainly due association of El Niño years with suppressed precipitation (Fig.1d). This non-linear relationship should explain the weak correlation between the MCT intensity and precipitation despite significant correlations between the MCT intensity and ENSO and between ENSO and precipitation.

For more detailed analysis on the MCT intensity, we made composite anomalies of global moisture flux, moisture flux divergence and precipitation for summers when MCT is stronger than normal (PC1_SLP < –1) (1981, 1987+, 1992+, 1995+, 1998+, 2016+, 2017) and when MCT is weaker (PC1_SLP > 1) (1984–, 1985–, 2007, 2011–, 2012–, 2021–), respectively. Years with "+" and "–" are for El Niño and La Niña years, respectively.

Figure 2 summarizes the composite analysis on the variability of the MCT intensity. In summers with the weakened MCT, an anticyclonic anomaly over the central MC, represents MCT weakening, accompanies anomalous moisture flux divergence and reduction of precipitation mainly in the central region of Mozambique (Figs. 2a, c). Contrarily, in summers with the strengthened MCT, a cyclonic anomaly prevails over the

MC and anomalous moisture flux convergence is seen in part of Mozambique (Fig. 2b). However, there is no significant precipitation anomaly in Mozambique (Fig. 2d). Those precipitation anomalies are consistent with no significant correlation of the MCT intensity with regional precipitation in Mozambique (Table 1). A composite analysis for SST anomalies shows that the weakened (strengthened) MCT is accompanied by warm (cool) SST anomalies over the central Pacific while there are no significant anomalies over the subtropical Indian Ocean (not shown). This is also consistent with the significant correlation of the MCT intensity with the NINO3.4 index and with no significant correlation of that with the SIOD index.

To investigate the impact of the zonal shift of the MCT, we selected summers with the westward shift of the MCT (PC2_SLP > 1) (1981, 1991, 1993, 1997, 1999–, 2006–, 2017, 2021–). We also selected summers with the eastward shift of the MCT (PC2_SLP < –1) (1989–, 1994, 1998+, 2008–, 2016+, 2018–, 2020). The correlation between PC2_SLP and the SIOD index is significantly positive (Table 1). However, the SIOD index is not always positively (negatively) large associated with large value of positive (negative) PC2_SLP (Fig.1d). Thus, we further considered summers when the westward shift of the MCT accompanied the positive SIOD (i.e., PC2_SLP > 1 and SIOD > 0.5) (1981, 1993, 1999–, 2006–, 2017). We also considered summers when the eastward shift of the MCT accompanied the negative SIOD (i.e., PC2_SLP < –1 and SIOD < –0.5) (1992+, 1998+, 2016+, 2020).

The westward shift of the MCT tends to accompany cool SST anomalies over the tropical Pacific suggestive of La Niña, a dipole pattern of SST anomalies over the subtropical South Atlantic, another dipole pattern over the subtropical Indian Ocean similar to the positive SIOD, and cooler SSTs over the tropical Indian Ocean (Fig. 3a).

Almost the same SST anomaly pattern is seen in composited anomalies associated with the westward-shifted MCT with the positive SIOD (Fig. 3c). It is noteworthy that the two dipole patterns in the subtropical Atlantic and Indian Oceans are reminiscent of the SST anomaly pattern associated with increase of precipitation averaged over Southern Africa (Morioka et al. 2012).

In contrast, the eastward shift of the MCT does not accompany SST anomalies in the tropics. There is only a hint of the negative SIOD in the subtropical Indian Ocean (Fig. 3b). However, if the eastward shift of the MCT is accompanied by the negative SIOD, warm SST anomalies appear in the tropical Pacific suggesting El Niño (Fig. 3d). In fact, three out of four years are El Niño. In addition, warm SST anomalies are seen over the subtropical Indian Ocean that have projection onto the negative SIOD. These results suggest that although the NINO3.4 index is not significantly correlated to PC2_SLP (Table 1), La Niña is associated with the westward shift of the MCT. And El Niño is associated with the eastward shift of the MCT if the negative SIOD accompanies the shift.

A composite map of SLP for summers with the westward-shifted MCT show a negative anomaly over southern and central Mozambique and a positive anomaly over the western coast of Madagascar and eastern MC, consistently with the westward shift of the MCT (Fig. 4a). In addition, negative anomalies over Angola and Namibia in southwestern Africa suggests strengthened and southward-shifted AL, and positive anomalies over the Indian Ocean suggests strengthened and zonally expanded MH. Those SLP anomalies accompany anomalous westward moisture fluxes from the Indian Ocean and eastward fluxes from the inland South Africa, which should lead to enhancement of moisture flux convergence and increase in precipitation in southern and central regions in Mozambique (Fig. 4a, Fig. 5a). These SLP and moisture flux anomalies are consistent with Crétat et al.

(2019), Pascale et al. (2019), and Xulu et al. (2020) that investigated the association of variability of the AL and MH with moisture flux convergence and precipitation anomalies over southern Africa. In northern Mozambique, anomalous moisture flux divergence and decreased precipitation are observed.

A similar circulation pattern is seen when the westward shift of the MCT is accompanied by the positive SIOD (Fig. 4c). But the anomalous moisture flux convergence in southern Mozambique and divergence in northern Mozambique are somewhat strengthened, which may slightly enhance precipitation anomalies in respective regions (Fig. 5c). It is noteworthy that a composite map similar to Fig. 4c, but only with neutral ENSO years (1981, 1993, 2017) shows almost the same circulation anomalies with Fig. 4c (not shown). This suggests that intensification of the AL and MH can occur even without influence from ENSO.

The patterns of SLP and moisture flux anomalies during summers with the eastward shift of the MCT (Fig. 4b) show almost the mirror images of those with the westward shift of the MCT (Fig. 4a). The pattern of precipitation anomalies in Mozambique is also almost the mirror image (Fig. 5b). When the eastward shift of the MCT is accompanied by the negative SIOD, the amplitudes of SLP and moisture flux anomalies are larger (Fig. 4d) compared to summers with the eastward shift of the MCT regardless of the SIOD phase (Fig. 4b). In particular, the positive SLP anomaly is dominant over the southern and central regions of Mozambique, which should cause even larger divergence anomaly of moisture flux and less precipitation there (Fig. 5d).

It should be noted that the moisture flux anomaly associated with the westward shift of the MCT is not necessarily a mirror image of that associated with the eastward shift over the subtropical Indian Ocean, particularly when SIOD events accompany (Figs 4c, d).

This should be due to asymmetry in wind anomalies between the westward and eastward shift (not shown). The reason for this asymmetry should be future work.

3. Conclusion and Discussion

To investigate the relationship between the MCT and regional precipitation variability in Mozambique in austral summer, we have applied the EOF analysis for interannual variability of DJF-mean SLP over the central MC. It was demonstrated that the dominant EOF mode (EOF1) represented intensity variability of the MCT and was significantly correlated to ENSO. However, it did not accompany regional precipitation variability in Mozambique. The zonal shift of the MCT, which was represented by the second EOF mode and has not been investigated in previous studies, was not correlated to ENSO. Rather, it was substantially associated with the SIOD and accompanied precipitation variability of southern, central, and northeastern regions of Mozambique. We particularly focused on the second mode as our main interest is precipitation in Mozambique.

The westward shift of the MCT accompanied intensification of the MH and AL, enhancing precipitation in southern and central regions while suppressing it in the northeastern region through anomalous moisture flux convergence. These precipitation anomalies can be strengthened when the positive SIOD occurred simultaneously with the westward-shifted MCT. SLP and precipitation anomalies accompanying the eastward shift of the MCT were almost mirror images of those during the westward shift of the MCT. If the eastward shift of the MCT accompanied the negative SIOD, those precipitation anomalies were enhanced and a statistically significant positive SST anomaly appeared over the central Pacific Ocean, which suggests El Niño and the negative SIOD might significantly affect the precipitation anomalies during the eastward

shift of MCT.

Unlike Barimalala et al. (2018, 2020) who examined the MCT variability in JFM-mean season when is the peak of its intensity, we investigated that in DJF-mean season. This is because our focus is on precipitation across Mozambique whose maximum is during DJF season. It should also be noted that Barimalala et al. (2018, 2020) were based on 850-hPa relative vorticity and geopotential over the MC, whereas we employed SLP in this study. Our findings were thus not necessarily consistent with those of Barimalala et al. (2020). We here discuss differences of our indices from theirs. They used area averages of 850-hPa relative vorticity (Vort_ave) and geopotential height (Geo_ave) over (16–26°S, 35–44°E). They also used the principal component of the first EOF of 850-hPa relative vorticity over the same domain (hereafter referred to as PC1_Vort). We thus repeated the correlation analysis mentioned above but with different indices that represent the MCT variability (Table 1). The first EOF of relative vorticity represents the MCT intensity whereas the second EOF represents northeast-southwest displacement of the MCT (not shown). The correlation coefficient of Vort_ave with the precipitation in the south is positive whereas that with the precipitation in the northeast is negative. This tendency is also observed in the correlation coefficients of PC1_Vort and PC2_Vort with precipitation in those regions. This suggests that those indices based on relative vorticity do not necessarily distinguish the MCT variability related to precipitation in Mozambique. We further calculated correlation coefficients of indices based on 850-hPa geopotential height. Those are similar to correlation coefficients based on SLP. Although relative vorticity is dynamically more relevant, we used SLP-based indices in this study because SLP-based indices should be easier for weather forecasters to handle than those based on relative vorticity and geopotential height.

In this study, we only show statistical relationship of the SIOD with the MCT and precipitation variability. Changes of the Mascarene High might cause those of the MCT as well as SIOD. Some studies, however, suggest SIOD impact on precipitation over the southern Africa through atmospheric general circulation model experiments (e.g., Reason 2001; 2002). Further study is needed to clarify the causal relationship among SIOD, MCT, and precipitation in Mozambique. In addition, we should keep in mind that Morioka et al. (2012) suggests that the SST dipole pattern in the subtropical South Atlantic, which appears associated with the westward shift of the MCT (Fig. 3a), may be more important than the SIOD for precipitation variability over Southern Africa. In addition, we only discussed seasonal-mean fields.

	Prec_Sout	Prec_Cent	Prec_NE	Prec_NW	Nino 3.4	SIOD
PC1_SLP	0.13	0.24	0.04	0.11	-0.57*	0.03
PC2_SLP	0.71*	0.51*	-0.64*	-0.10	-0.25	0.46*
Slp_ave	-0.15	-0.25	-0.03	-0.11	0.57*	-0.04
PC1_Vort	0.46*	0.25	-0.50*	-0.23	-0.01	0.35*
PC2_Vort	0.52*	0.31	-0.30	0.08	-0.33	0.27
Vort_ave	0.37*	0.18	-0.44*	-0.25	0.02	0.30
PC1_geo	-0.03	0.14	0.18	0.10	-0.55*	-0.03
PC2_geo	0.70*	0.58*	-0.61*	-0.06	-0.38*	0.42*
Geo_ave	0.01	-0.15	-0.16	-0.09	0.56*	0.02

Table 1. Simultaneous correlations of indexes representing MCT variability (see the main text for details) with regional precipitation in south, central, northeastern, and northwestern Mozambique. Correlations with Nino3.4 and SIOD are also shown. Asterisks indicate correlations being statistically significant at the 5% level with Student's t-test.

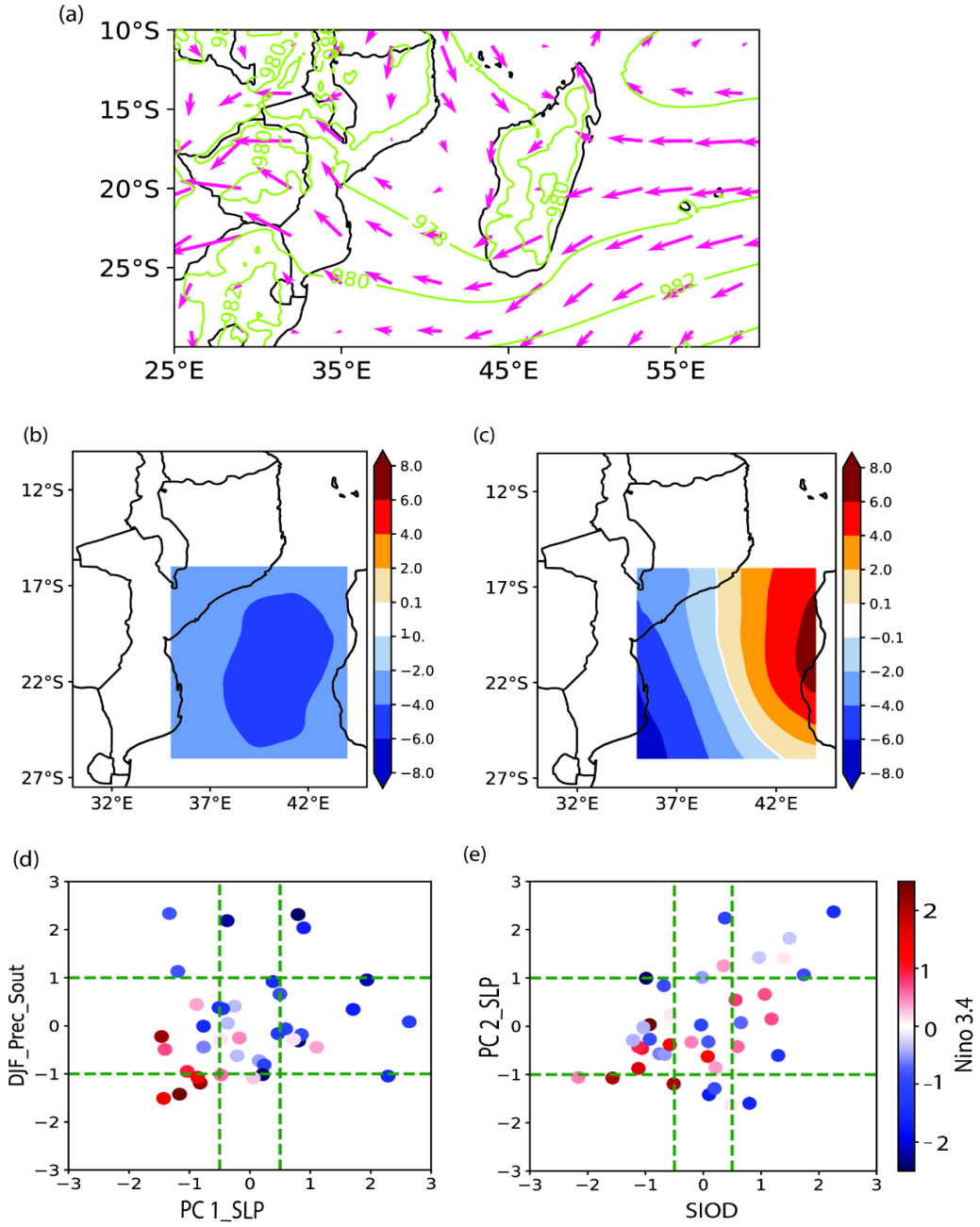

Fig. 1 (a) Climatological-mean 850-hPa moisture flux (arrow: g/kg m/s) and SLP (contour: hPa) for DJF over 1981−2021, (b,c) The (b) first and (c) second EOF modes of DJF-mean SLP over the MCT domain (35–44°E, 16–26°S) (arbitrary units), (d) scatter plot of PC1 and southern DJF-mean precipitation index and (e) scatter plot of PC2 and SIOD index with colors representing the NINO3.4 index (1981-2021).

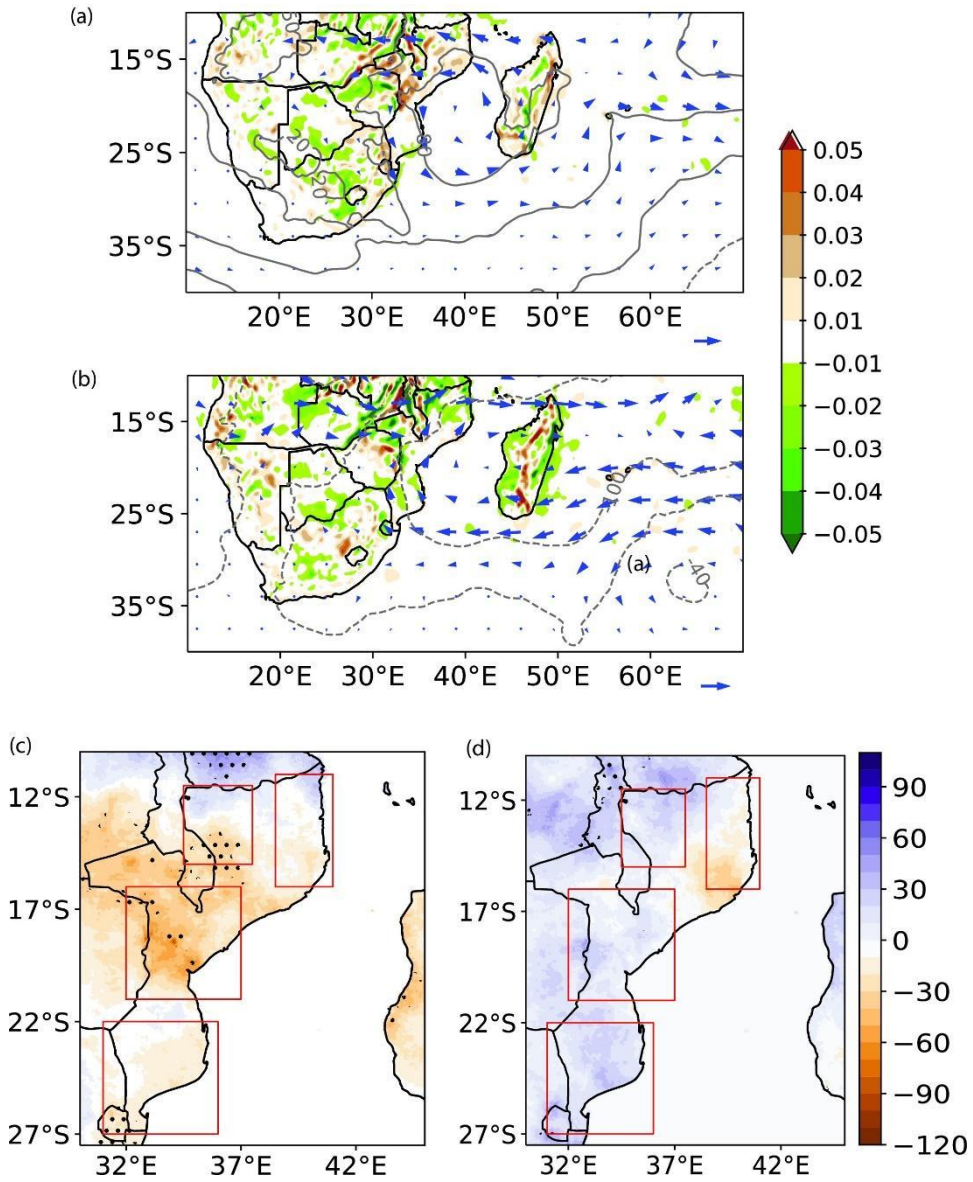

Fig. 2 Composite anomalies of DJF-mean SLP, moisture flux, and moisture flux divergence for summers with (a) weaker MCT (b) enhanced MCT. (c,d) As in (a) and (b), respectively, but for precpitation. Black dots indicate a statistically significant difference at the 10% level. Red squares in (c) and (d) signify northeastern, northwestern, central, and southern regions for averaging precipitation.

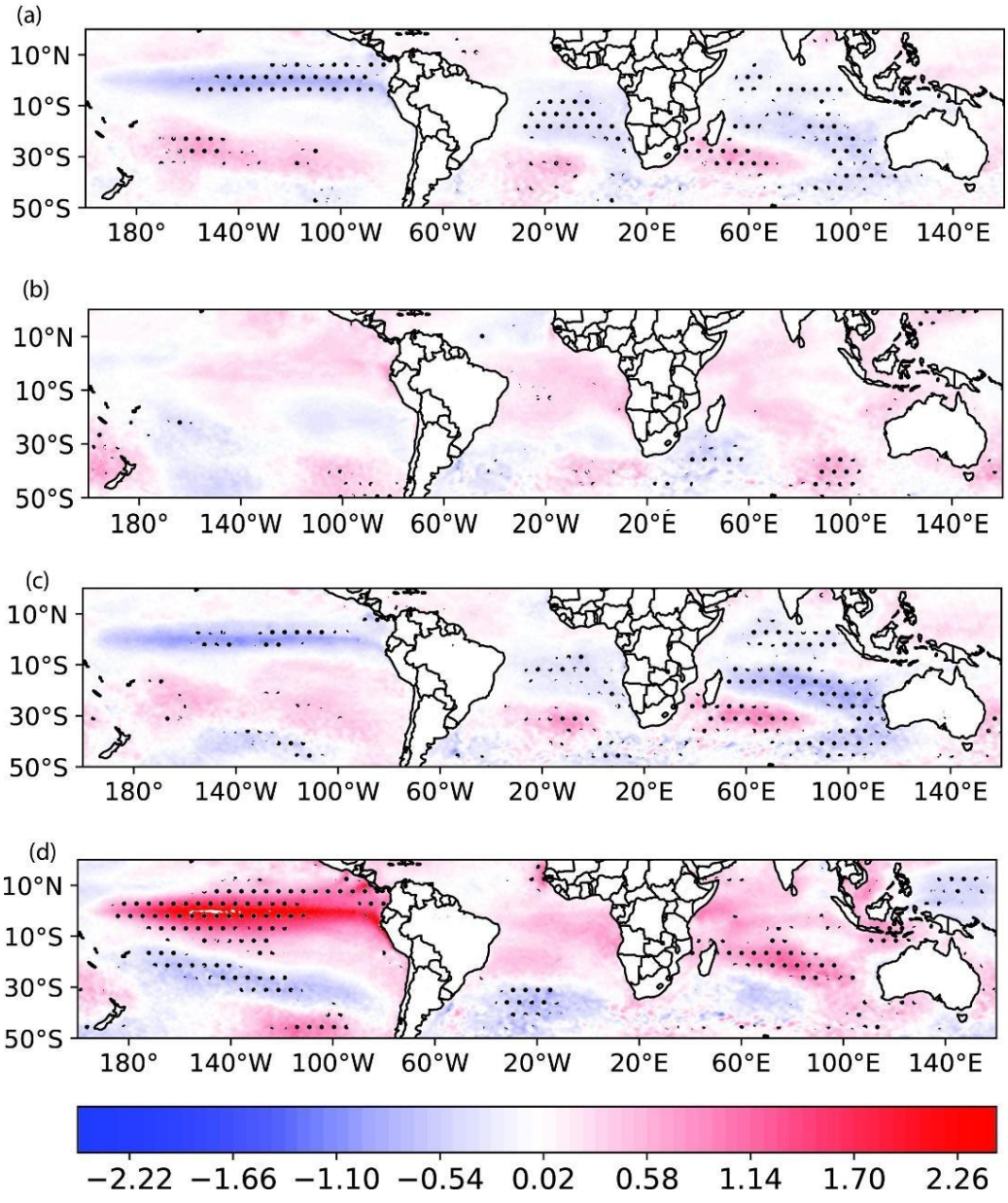

Fig. 3 Composited anomalies of DJF-mean SSTs for summers with (a) westward shift of MCT, (b) eastward shift of MCT, (c) westward-shifted MCT with positive SIOD, and (d) eastward-shifted MCT with negative SIOD. Black dots indicate a statistically significant difference at the 10% level.

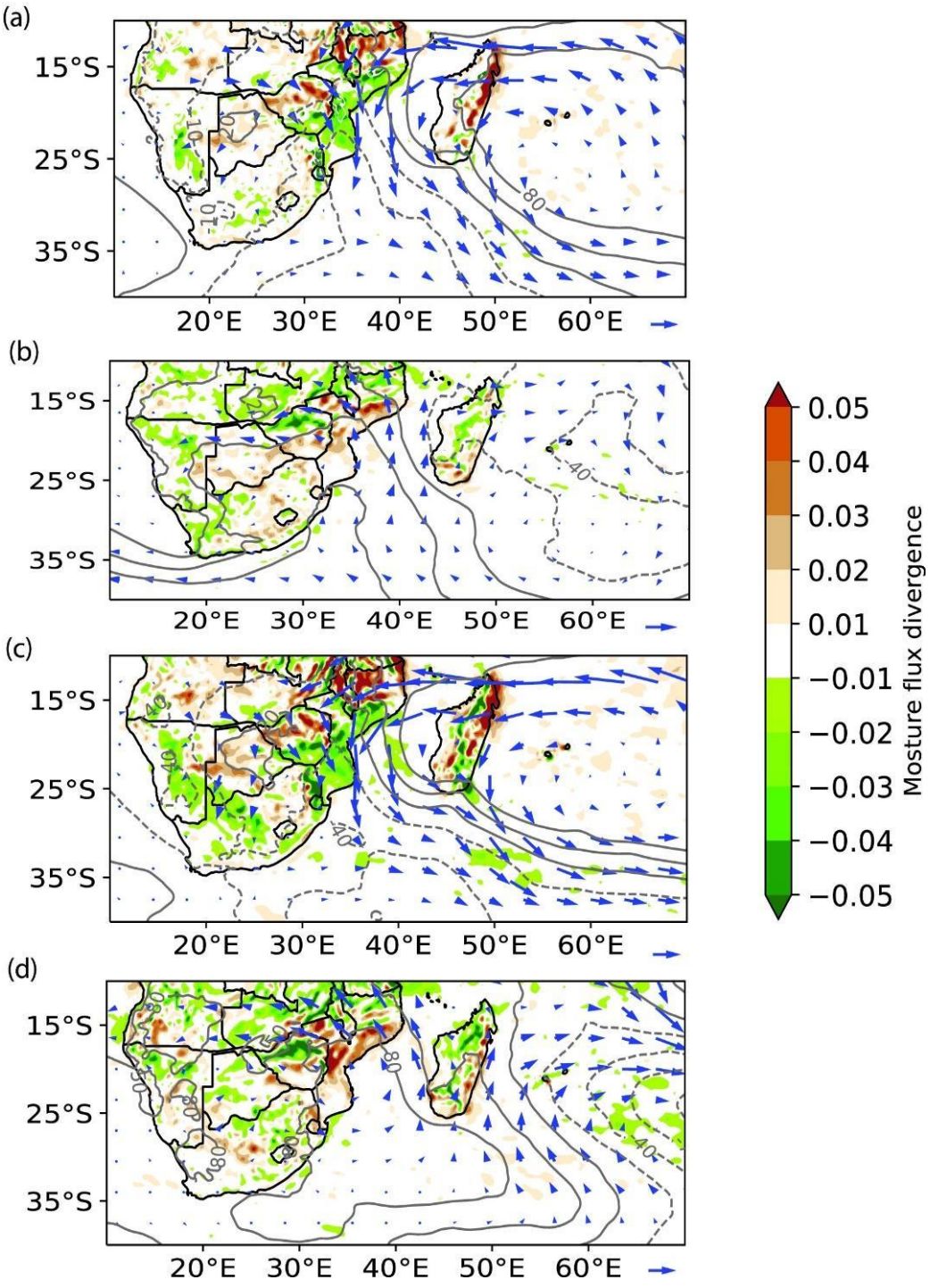

Fig. 4 Same as Fig. 3 but for SLP (counter), 850-hPa moisture flux divergence (shaded) and moisture flux (10^{-4} Kg m^{-2} s^{-1}, black arrows).

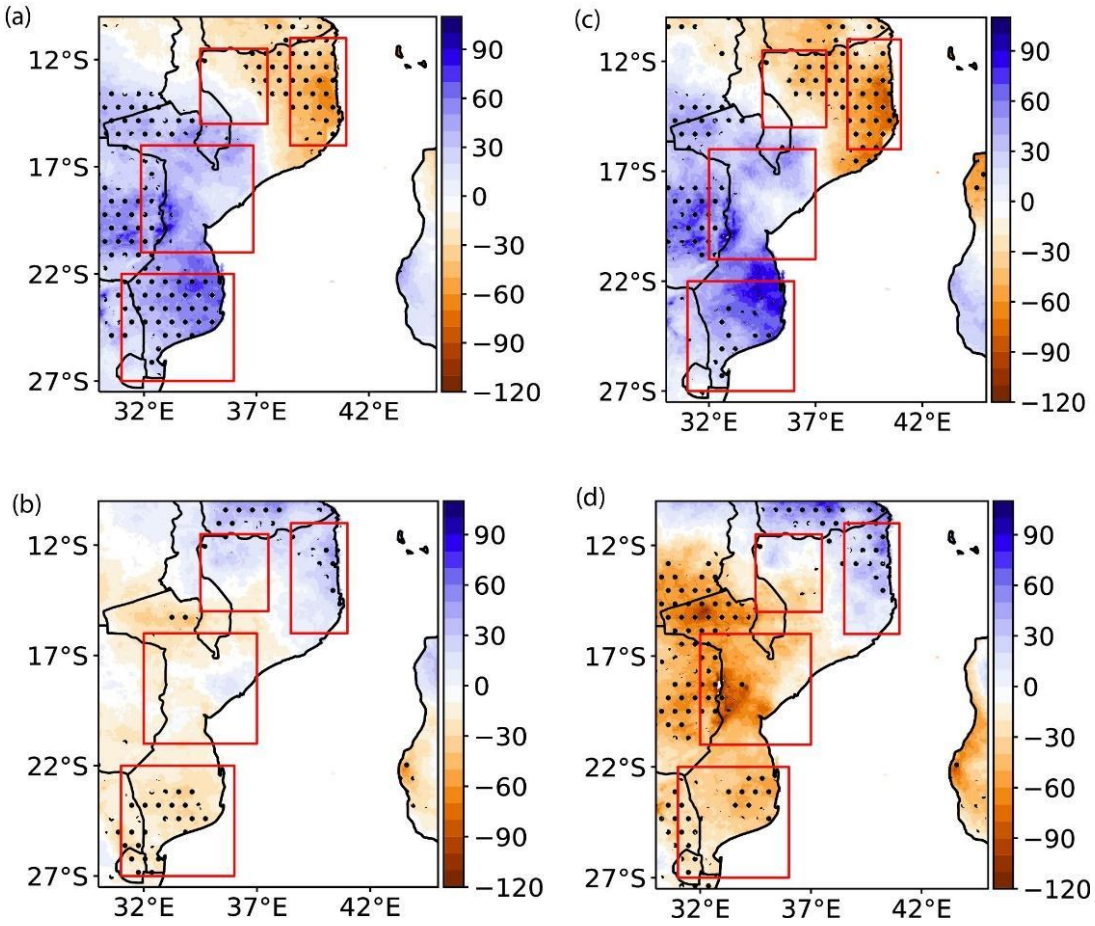

Fig. 5 Same as Fig. 3 but for precipitation. The four marked domains represent four precipitation regions (southern, central, northwest, and northeast) in Mozambique.

CHAPTER IV

General Conclusions

La Niña (El Niño), and negative (positive) phases of IOD tend to precede above- (below-) normal precipitation in central and southern regions of Mozambique by one season. The negative (positive) Niño 1.2 index tends to precede precipitation above (below) normal only in the central region by one season. With a lead time of two seasons, La Niña (El Niño) and positive (negative) phases of Benguela Niño exhibited robust associations with above- (below-) normal precipitation in southern and central regions.

The northwestern and northeastern regions were less affected by modes of climate variability where positive (negative) IOD in preceding SON season was significantly associated with precipitation above (below) normal in the northeastern region, while in the northwestern region, only the negative (positive) phase of Benguela Niño was significantly associated with precipitation above (below) normal with a lead time of two seasons.

In atypical La Niña and El Niño events, which did not accompany precipitation anomalies in southern and central Mozambique, there was also Rossby wave propagation over the South Pacific as in typical ENSO events, but it did not reach the South Atlantic and South Africa, resulting in normal precipitation in southern and central regions.

The SIOD did not lead regional DJF precipitation at any season but, was substantially associated with the zonal shift of MCT and accompanied precipitation variability in southern, central, and northeastern regions of Mozambique. The westward shift of the MCT accompanied intensification of the MH and AL, enhancing precipitation in southern and central regions while suppressing it in the northeastern region through anomalous moisture flux convergence. These precipitation anomalies can be strengthened when the positive SIOD

occurred simultaneously with the westward-shifted of MCT.

On the other hand, if the eastward shift of the MCT, which is almost a mirror image of the westward shift, accompanied the negative SIOD, those precipitation anomalies were enhanced and a statistically significant, positive SST anomaly appeared over the central Pacific Ocean, which suggests El Niño and the negative SIOD might significantly affect the precipitation anomalies during the eastward shift of MCT.

References

Barimalala, R., James, R., Munday, C. & Reason, C.J.C. (2022) Representation of the Mozambique channel trough and its link to southern African rainfall in CMIP6 models. *Climate Dynamics*. https://doi.org/10.1007/s00382-022-06480-1.

Barimalala, R., Desbiolles, F., Blamey, R. C. & Reason, C. (2018) Madagascar influence on the South Indian Ocean Convergence Zone, the Mozambique Channel Trough and southern African rainfall. *Geophys. Res. Lett.*, **45**, 11 380–11, 389, https://doi.org/10.1029/2018GL079964.

Barimalala, R., Blamey, R. C., Desbiolles, F. & Reason, C. J. C. (2020) Variability in the Mozambique Channel Trough and Impacts on Southeast African Rainfall. *J. Climate*, 33, 749–765. https://doi.org/10.1175/JCLI-D-19-0267.1.

Behera, S.K., Luo, J.J., Masson, S., Rao, S.A., Sakuma, H. & Yamagata, T. (2006) A CGCM Study on the Interaction between IOD and ENSO. *Journal of Climate*, 19, 1688–1705. https://doi.org/10.1175/JCLI3797.1.

Behera, S.K., Morioka, Y., Ikeda, T., Doi, T., Ratnam, J.V., Nonaka, M. et al. (2018) Malaria incidences in South Africa linked to a climate mode in southwestern Indian Ocean. *Environmental Development,* 27, 47–57. https://doi.org/10.1016/j.envdev.2018.07.002.

Behera, S.K. & Yamagata, T. (2001) Subtropical SST dipole events in the southern Indian Ocean. *Geophysical Research Letters*, 28, 327–330. https://doi.org/10.1029/2000GL011451.

Blamey, R.C. & Reason, C.J.C. (2023) Diversity and Ranking of ENSO Impacts along the Eastern Seaboard of Subtropical Southern Africa. *Atmosphere* 14, 6: 1042. https://doi.org/10.3390/atmos14061042

Bozzola, M., Massetti, E., Mendelsohn, R. & Capitanio, F. (2018) A Ricardian analysis of the impact of climate change on Italian agriculture. *European Review of Agricultural Economics,* 45, 57–79. https://doi.org/10.1093/erae/jbx02.

Camberlin, P., Janicot, S. & Poccard, I. (2001) Seasonality and atmospheric dynamics of the teleconnection between African rainfall and tropical sea-surface temperature: Atlantic vs. ENSO. *International Journal of Climatology*, 21, 973-1005. https://doi.org/10.1002/joc.673.

Chongue, L. A. & Nishii, K. (2024) The influence of tropical and subtropical modes of climate variability on precipitation in Mozambique. *Int. J. Climatol.*, 1–13. https://doi.org/10.1002/joc.8509.

Colberg, F., Reason, C.J.C. & Rodgers, K. (2004) South Atlantic response to El Niño–Southern Oscillation induced climate variability in an ocean general circulation model, *J. Geophys. Res.*, 109, C12015, https://doi.org/10.1029/2004JC002301

Cook, K.H. (2000) The South Indian Convergence Zone and Interannual Rainfall Variability over Southern Africa. *Jornal of Climate*, 13, 3789–3804. https://doi.org/10.1175/1520-0442(2000)013<3789:TSICZA>2.0.CO;2

Cook, K. H. (2001) A Southern Hemisphere wave response to ENSO with implications for Southern Africa precipitation. *J. Atmos. Sci.*, **58**, 2146–2162, https://doi.org/10.1175/1520-0469(2001)058<2146:ASHWRT>2.0.CO;2.

Crétat, J., Pohl, B. & Dieppois, B. (2019) The Angola Low: relationship with southern African rainfall and ENSO. *Clim. Dyn.,* **52**, 1783–1803. https://doi.org/10.1007/s00382-018-4222-3.

Driver, P. & Reason, C.J.C. (2017) Variability in the Botswana High and its relationships with rainfall and temperature characteristics over southern Africa. *International*

Journal of Climatology, 37, 570–581. https://doi.org/10.1002/joc.5022.

Eckstein, D., Kunzel, V. & Schafer, L. (2021) Global climate risk index 2021. Who suffers most from extreme weather events? Weather-Related Loss Events in 2019 and 2000-2019. Germanwatch. [Cited 2023 July 16] Available from: http://www.germanwatch.org/en/cri.

Florenchie, P., Lutjeharms, J.R.E., Reason, C.J.C., Masson, S. & Rouault, M. (2003) The source of Benguela Ninõs in the South Atlantic Ocean. *Geophysical Research Letters*, 30, 10–13. https://doi.org/10.1029/2003GL017172.

Funk, C., Peterson, P., Landsfeld, M., Pedreros, D., Verdin, J., Shukla, S. et al. (2015) The climate hazards infrared precipitation with stations — a new environmental record for monitoring extremes. *Science Data* 2, 150066. https://doi.org/10.1038/sdata.2015.66.

Gaughan, A.E., Staub, C.G., Hoell, A., Weaver, A. & Waylen, P.R. (2016) Inter- and intra-annual precipitation variability and associated relationships to ENSO and the IOD in southern Africa. *International Journal of Climatology*, 36, 1643–1656. https://doi.org/10.1002/joc.4448.

Harp, R.D., Colborn, J.M., Cadrinho, B., Kathryn, L.C., Zhang, L. & Karnauskas, K.B. (2021) Interannual climate variability and malaria in Mozambique. *GeoHealth*, 5, e2020GH000322. https://doi.org/10.1029/2020GH000322.

Harp, R. D., J. M. Colborn, B. Cadrinho, L.C. Kathryn, L. Zhang, and K. B. Karnauskas, 2020: Interannual climate variability and malaria in Mozambique. *GeoHealth*, **5**, e2020GH000322. https://doi.org/10.1029/2020GH000322.

Harrison, M. S. J. (1984) A generalized classification of South African summer rain-bearing Systems. *J. Climate,* **4***,* 1-13. https://doi.org/10.1002/joc.3370040510.

Hersbach, H., Bell1, B., Berrisford, P., Hirahara, S., Horányi, A., Muñoz-Sabater *et al.* (2020) The ERA5 global reanalysis. *Quarterly Journal of the Royal Meteorological Society*, 146, 1999–2049. https://doi.org/10.1002/qj.3803.

Imbol Koungue, R. A., Illig, S. & Rouault, M. (2017) Role of interannual Kelvin wave propagations in the equatorial Atlantic on the Angola Benguela Current system, *Journal of Geophysical Reseach. Oceans*, 122, 4685–4703, doi:10.1002/2016JC012463.

Imbol Koungue, R.A., Rouault, M., Illig, S., Brandt, P. & Jouanno, J. (2019) Benguela Niños and Benguela Niñas in forced ocean simulation from 1958 to 2015. *Journal of Geophysical Research: Oceans*, 124, 5923–5951. https://doi.org/10.1029/2019JC015013

Jury, M.R. & Huang, B. (2004) The Rossby wave as a key mechanism of Indian Ocean climate variability. *Deep-Sea Research I*, 5, 2123–2136. https://doi.org/10.1016/j.dsr.2004.06.005.

Koseki, S. & Koungue, R.A.I. (2020) Regional atmospheric response to the Benguela Niñas. *International Journal of Climatology*, 41, E1483-E1497. https://doi.org/10.1002/joc.6782.

Kruger, A.C. (1999) The influence of the decadal-scale variability of summer rainfall on the impact of El Niño and La Niña events in South Africa. *International Journal of Climatology*, 19, 59-68. https://doi.org/10.1002/(SICI)1097-0088(199901)19:1<59:AID-JOC347>3.0.CO;2-B.

Love, T.B., Kumar, V., Xie, P. & Thiaw, W. (2004) A 20-year daily Africa precipitation climatology using satellite and gauge data. In Proceedings of the 84th AMS Annual Meeting, vol. Conference on Applied Climatology, Seattle.

Lübbecke, J.F., Böning, C.W., Keenlyside, N.S. & Xie S.-P. (2010) On the connection between Benguela and equatorial Atlantic Niños and the role of the South Atlantic Anticyclone, *Jornal of Geophysical Reseach*, 115, C09015, doi:10.1029/2009JC005964.

Machaieie, H.A., Silva, C.G., Oliveira, E.N. de, Júnior, H.I.T. & Almeida, H.A. (2020) Variability and trends of precipitation in Quelimane, Central Mozambique, and their relation to El Niño Southern Oscillation. *Journal of Geoscience and Environment Protection*, 8, 1–16. https://doi.org/10.4236/gep.2020.87001.

Manatsa, D. & Mukwada, G. (2012) Rainfall mechanisms for the dominant rainfall mode over Zimbabwe relative to ENSO and/or IODZM. *The Scientific World Journal,* 2012, Article ID 926310. https://doi.org/10.1100/2012/926310.

Manhique, A.J., Reason, C.J.C., Rydberg, L. & Fauchereau, N. (2011) ENSO and Indian Ocean sea surface temperatures and their relationships with tropical temperate troughs over Mozambique and the Southwest Indian Ocean. *International Journal of Climatology*, 31, 1-13. https://doi.org/10.1002/joc.2050.

Manhique, A.J., Reason, C.J.C., Silinto, B., Zucula, J., Raiva, I., Congolo, F. & Mavume, A.F. (2015) Extreme Rainfall and Floods in Southern Africa in January 2013 and Associated Circulation Patterns. *Natural Hazards*, 77, 679-691. https://doi.org:10.1007/s11069-015-1616-y.

Mavume, A.F., Rydberg, L., Rouault, M. & Lutjeharms, J.R.E. (2009) Climatology and landfall of tropical cyclones in the Southern West Indian Ocean. *Western Indian Ocean Journal of Marine Science*, 8,15-36. https://doi.org/10.4314/wiojms.v8i1.56672

McHugh, M.J. (2006) Impact of South Pacific circulation variability on east African

rainfall.*International Journal of Climatology*, 26, 505-521. https://doi.org/10.1002/joc.1257.

Meque, A. & Abiodun, B.J. (2015) Simulating the link between ENSO and summer drought in Southern Africa using regional climate models. *Climate Dynamics*, 44, 1881–1900. https://doi.org/10.1007/s00382-014-2143-3.

Moihamette, F., Pokam, W.M., Diallo, I. & Washington, R. (2022) Extreme Indian Ocean dipole and rainfall variability over Central Africa. *International Journal of Climatology*, 42, 5255– 5272. https://doi.org/10.1002/joc.7531

Morioka, Y., Tozuka, T., Masson, S., Terray, P., Luo, J.-J. & Yamagata, T. (2012) Subtropical dipole modes simulated in a coupled general circulation model. *J. Climate,* **25**, 4029-4047. https://doi.org/10.1175/JCLI-D-11-00396.1.

Morioka, Y., Tozuka, T. & Yamagata, T. (2011) On the growth and decay of the subtropical dipole mode in the South Atlantic. *Journal of Climate*, 24, 5538–5554. https://doi.org/10.1175/2011JCLI4010.1.

Mulenga, H. M., Rouault, M. & Reason, C.J.C. (2003) Dry summers over northeastern South Africa and associated circulation anomalies. *Climate Research*, 25, 29–41. https://doi.org/10.3354/cr025029.

Nicholson, S.E. (2000) The nature of rainfall variability over Africa on time scales of decades to millennia. *Global and Planetary Change*, 26, 137-158.

Nicholson, S.E. (2018) The ITCZ and the Seasonal Cycle over Equatorial Africa. *Bulletin of the American Meteorological Society,* **99**, 337–348. https://doi.org/10.1175/BAMS-D-16-0287.1.

Ninomiya, K. (2008) Similarities and Differences among the South Indian Ocean Convergence Zone, North American Convergence Zone, and Other Subtropical

Convergence Zones Simulated Using an AGCM. *Journal of the Meteorological Society of Japan*, 86, 141-165. https://doi.org/10.1016/S0924-7963(00)00085-3.

O'Brien, K. & Vogel, C. (2003) Coping with climate variability: the use of seasonal climate forecasts in Southern Africa. Routledge, 220 pp. https://doi.org/10.1016/S0921-8181(00)00040-0.

Pascale, S., Pohl, B., Kapnick, S.B. & Zhang, H. (2019) On the Angola low interannual variability and its role in modulating ENSO effects in southern Africa. *Journal of Climate*, 32, 4783–4803. https://doi.org/10.1175/JCLI-D-18-0745.1.

Ratnam, J.V., Behera, S.K., Masumoto, Y. & Yamagata, T. (2014) Remote effects of El Niño and Modoki events on the austral summer precipitation of Southern Africa. *Journal of Climate*, 27, 3802–3815. https://doi.org/10.1175/JCLI-D-13-00431.1.

Rauniyar, S.P. & Walsh, K.J.E. (2013) Influence of ENSO on the diurnal cycle of rainfall over the Maritime Continent and Australia. *Journal of Climate,* 4, 1304–1321. https://doi.org/10.1175/JCLI-D-12-00124.1.

Reason, C. J.C. & Jagadheesha, D. (2005) A model investigation of recent ENSO impacts over southern Africa. *Meteorology and Atmospheric Physics,* 89,181–205. https://doi.org/10.1007/s00703-005-0128-9.

Reason, C. J. C. (2001) Subtropical Indian Ocean SST dipole events and southern African rainfall, *Geophys. Res. Lett.*, **28**, 2225-2228. https://doi.org/10.1029/2000GL012735.

Reason, C. J. C. (2002) Sensitivity of the southern African circulation to dipole sea-surface-temperature patterns in the south Indian Ocean. *Int. J. Climatol.*, **22**. 377-393. https://doi.org/10.1002/joc.744.

Reason, C. J.C., Landman, W. & Tennant, W. (2006) Seasonal to decadal prediction

of southern African climate and its links with variability of the Atlantic Ocean. *Bulletin of the American Meteorological Society*, 87, 941–955. https://doi.org/10.1175/BAMS-87-7-941.

Reason, C.J.C. & Mulenga, H. (1999) Relationships between South African rainfall and SST anomalies in the southwest Indian Ocean. *International Journal of Climatology,* 19, 1651–1673. https://doi.org/10.1002/(SICI)1097-0088(199912)19:15%3C1651::AID-JOC439%3E3.0.CO;2-U

Reason, C.J.C. & Smart, S. (2015) Tropical southeast Atlantic warm events and associated rainfall anomalies over southern Africa. *Frontiers Environmental Science,* 3:24. https://doi.org/10.3389/fenvs.2015.00024

Ropelewski, C.F. & Halpert, M.S. (1987) Global and regional scale precipitation patterns associated with the El Niño/Southern Oscillation. *Monthly Weather Review*, 115, 1606-1626. https://doi.org/10.1175/15200493(1987)115<1606:GARSPP>2.0.CO;2.

Saji, N. H., Goswami, B.N., Vinayachandran, P.N. & Yamagata T. (1999) A dipole mode in the tropical. Indian Ocean. *Nature*, 40,1360-3. https://doi.org/10.1038/43854.

Saji, N.H. & Yamagata, T. (2003) Possible impacts of Indian Ocean Dipole mode events on global climate. *Climate Research*, 25, 151–169. http://www.jstor.org/stable/24868393.

Shannon, L.V., Boyd, A.J., Brundrit, G.B. & Taunton-Clark, J. (1986) On the existence of an EI Niño-type phenomenon in the Benguela System. *Journal of Marine Research*, 44, (3). https://elischolar.library.yale.edu/journal_of_marine_research/1826.

Takaya, K. & Nakamura, H. (2001) A formulation of a phase-independent wave-activity flux for stationary and migratory quasigeostrophic eddies on a zonally varying basic flow. *Journal of the Atmospheric Sciences,* 58, 608–627. https://doi.org/10.1175/1520-0469(2001)058<0608:AFOAPI>2.0.CO;2.

Tyson, P.D. & Preston-Whyte, R.A. (2000) The Weather and Climate of Southern Africa. Oxford University Press, 387 pp.

Washington, R. & Todd, M. (1999) Tropical–temperate links in southern African and Southwest Indian Ocean satellite-derived daily rainfall. *Int. J. Climatol.,* **19**, 1601-1616. https://doi.org/10.1002/(SICI)1097-0088(19991130)19:14<1601::AID-JOC407>3.0.CO;2-0.

Xulu, N.G., Chikoore, H., Bopape, M.-J. M. & Nethengwe, N. S. (2020) Climatology of the Mascarene High and its Influence on weather and climate over Southern Africa. *Climate*, *8*, 86. https://doi.org/10.3390/cli8070086.